Research Article

Kamal Shah, Shabir Ahmad, Aman Ullah, and Thabet Abdeljawad*

Study of chronic myeloid leukemia with T-cell under fractal-fractional order model

https://doi.org/10.1515/phys-2024-0032
received December 16, 2023; accepted April 25, 2024

Abstract: This research work is devoted to investigate myeloid leukemia mathematical model. We give some details about the existence of trivial and nontrivial equilibrium points and their stability. Also, local asymptotical stability of disease-free and endemic equilibrium points is discussed. Also, positivity of the solution has been discussed. Some sufficient results are achieved to study the local existence and uniqueness of solution to the considered model for Mittag–Leffler kernel using the Banach contraction theorem. Three numerical algorithms are derived in obtaining the numerical solution of suggested model under three different kernels using Adams–Basforth technique. Numerical results have been presented for different fractals and fractional orders to show the behavior of the proposed model.

Keywords: fractal-fractional operators, myeloid leukemia, model, Adams–Basforth method

*** Corresponding author: Thabet Abdeljawad**, Department of Mathematics and Sciences, Prince Sultan University, P.O. Box 66833, 11586 Riyadh, Saudi Arabia; Department of Medical Research, China Medical University, Taichung 40402, Taiwan; Department of Mathematics and Applied Mathematics, School of Science and Technology, Sefako Makgatho Health Sciences University, Ga-Rankuwa, South Africa, e-mail: tabdeljawad@psu.edu.sa
Kamal Shah: Department of Mathematics and Sciences, Prince Sultan University, P.O. Box 66833, 11586 Riyadh, Saudi Arabia; Department of Mathematics, University of Malakand, Chakdara, Dir Lower, Khyber Pakhtunkhwa, Pakistan, e-mail: kamalshah408@gmail.com, kshah@psu.edu.sa
Shabir Ahmad: Department of Mathematics, University of Malakand, Chakdara, Dir Lower, Khyber Pakhtunkhwa, Pakistan, e-mail: shabirahmad2232@gmail.com
Aman Ullah: Department of Mathematics, University of Malakand, Chakdara, Dir Lower, Khyber Pakhtunkhwa, Pakistan, e-mail: amanswt@gmail.com

1 Introduction

Abel first studied the notable application of fractional calculus (FC) in physics. In the same way, Riemann, Liouville, Lagrange, Hadmard, *etc*. have greatly contributed in this field [1]. Latter, different definitions were introduced by numerous researchers including Caputo, Fabrizio, Atangana and Baleanu, *etc*. Therefore, the area has given much more attention and also been applied to study various real-world problems. For some historical contributions in this regard, we refer to studies by AlBaidani *et al.* [2] and Ferrari *et al.* [3]. Recently, researchers have conducted many results for the existence theory and numerical solutions for different problems using fractional differential operators. Here, some significant contribution has been referred to previous studies [4–8]. Moreover, the use of FC in investigating different real-world process is an important area of research in recent times. Here, we refer some previous studies [9–13].

The different concepts of FC have been used in applied mathematics and proved to be a good operator for modeling any physical phenomena. Mostly, three types of operators are used in FC, which are based on three kernels, *i.e.*, power law, exponential, and the Mittag–Leffler-type kernels. Modeling and graphical visualization using these three types of kernels are heavily influenced by the study of fractional differential equations (here, we refer previous studies [14,15]). Mathematical models have been studied very well using fractional order derivatives [16–18]. For more details, see some contributions on the said area in previous studies [19–23]. Kumar *et al.* [24] studied the susceptible infected recovered susceptible malaria infection model under Caputo–Fabrizio operator. A non-integer-order biological model with the consideration carrying capacity is studied in by Srivastava *et al.* [25]. Furthermore, human immunodeficiency virus-1 infection model of CD4+ T-cells with effects of antiviral drug therapy in fractional operator sense was analyzed by Kumar *et al.* [26]. We include recent studies of FC in different applied sciences in Singh [27] and Ahamed *et al.* [28]. For further analysis, numerical results, and stability theory for various problems of FC, we refer to previous studies [29–33]. Also, researchers have derived some

appropriate results devoted to computational analysis of partial differential equations with Mittag–Leffler kernel as well as of some biological models. Readers can read the said work in previous studies [34–39].

Non-local derivatives, in general, are appropriate for such circumstances because, depending on whether there is a power law, fading memory, or crossover effects, they can preserve non-localities and also some memory effects. However, if more intricate behaviors cannot be replicated using a fading memory, crossover behavior, or power law, the recently developed fractals fractional derivative (FFD) operators may be more effective mathematical tools to cope with such behaviors [40]. The FFD operators have many applications in real-world problems. A non-Newtonian generalization of the derivative is the fractal derivative, which is often known as the Hausdorff derivative. This type of derivative was used to study a fluid flow problems in many studies. The FFD operators have recently attracted the attention of researchers very well. As the concept is still fresh, this area has to be studied. These new operators were introduced by Atangana: connecting the fractal calculus with FC [41]. Different complex behaviors were studied through these operators [42,43]. Also, recent contribution can be read in previous studies [44,45]. Compact in nature, fractal theory is a subfield of nonlinear science with important applications in turbulence, aquifers, porous media, and other media that typically display fractal qualities. When it comes to understanding concepts such as fractional-order integration and differentiation and their mutually inverse relationship, FC is crucial. Many branches of engineering and research, including electromagnetics, viscoelasticity, fluid mechanics, electrochemistry, biological population models, optics, and signal processing, use FC [46].

The most powerful tools to investigate real-world problems from mathematical perspectives are devoted to modeling. The said area has given much more attention in the last many decades. With the help of mathematical formulations, we easily understand about the transmission dynamics of the process. Keeping in mind the applications, researchers have increasingly used the said area to model various chronic diseases. In this regard, significant work has been performed using classical and fractional order derivatives. Here, for reference, we refer few articles [47–49].

Chronic myelogenous leukemia (CML or chronic granulocytic leukemia) is a cancer of white blood cells (WBCs). In CML, a wide range of WBCs are produced by bone marrow, which also affects cell in blood circulation. This form of leukemia is uncommon. Adults are more likely to acquire CML than youngsters. CML occurs when the myeloid cells are transformed into immature cancer cells through a genetic alteration. Such cells then expand slowly and overtake the healthy cells in bone marrow and blood [50] called translocation. In translocation, a chromosome 9 (called the ABL gene) breaks and makes bond with section of the chromosome 22 (called the BCR gene), forming a Philadelphia chromosome (Ph chromosome). Therefore, Ph chromosome is a bond of two genes (ABL and BCR) that forms a fusion of single gene BCR-ABL [51,52]. It is only found in blood-forming cells. It causes myeloid cells that make an abnormal activated tyrosine kinase enzyme known as fusion protein, which allows us to grow WBCs out of control [53,54]. The number of WBCs is normally regulated by the body; however, more WBCs are generated in stress or during infections, but after the recovery the numbers become normal. In CML, the abnormal BCR-ABL enzyme behaves as a switch stuck-in the on position, and it proceeds to promote the growth and multiplication of WBCs. In addition to increasing WBCs, there is also an increase in the number of blood platelets that help in blood clotting, and amount of red blood cells carrying oxygen can be decreased. Therefore, an irregular or an unusual amount of platelets or even RBC are seen in CML. The symptoms of CML may include easy bleeding, pain in bones, feeling full by eating some food, feeling tired, weight loss with no exercise, fever, fullness or pain below ribs on left side, loss of appetite, and very high sweating in sleep. CML has three phases, which are accelerated, chronic, and blastic. The information from tests and procedures performed to diagnose CML is also used to plan treatment. Due to huge amount of blast-cells in blood and bone marrow, space reduces for healthy WBC, RBC, and platelets, which causes anemia, infections, bleeding, bone pain, or a sensation of fullness under the left ribs. Blast cells in the bone marrow and blood as well as the intensity of symptoms will determine the disease stage. During chronic CML process, blast cells are less than 10% of the cells in bone marrow and blood. During the accelerated phase of CML, the blast cells are 10 to 19% of the blood cells and the bone marrow. Blast cells are 20% or more of the cells in bone marrow or blood in blastic process CML.

Here, it should be worth to mention that researchers have used the concepts of mathematical model to understand and investigate the transmission dynamics of the aforementioned disease properly. For instance, Moore and Li [55] applied the traditional calculus to construct the following model as

$$\begin{cases} \dfrac{\mathrm{d}\mathcal{T}}{\mathrm{d}t} = s_n - d_n\mathcal{T} - k_n\mathcal{T}\left(\dfrac{C}{C+\eta}\right), \\ \dfrac{\mathrm{d}\mathcal{E}}{\mathrm{d}t} = a_n k_n \mathcal{T}\left(\dfrac{C}{C+\eta}\right) + \alpha_e\mathcal{E}\left(\dfrac{C}{C+\eta}\right) - d_e\mathcal{E} - \gamma_e C\mathcal{E}, \\ \dfrac{\mathrm{d}C}{\mathrm{d}t} = r_c C \ln\left(\dfrac{C_{\max}}{C}\right) - d_c C - \gamma_c C\mathcal{E}, \end{cases} \tag{1}$$

Table 1: Nomenclature and their description

Nomenclature	Description
s_n	is the $\mathcal{T}$ source term
d_n	represents the $\mathcal{T}$ death rate
d_e	is the $\mathcal{E}$ death rate
d_c	represents the C death rate
k_n	represents the $\mathcal{T}$ differentiation
η	is the Michaelis–Menten coefficient
α_n	represents the $\mathcal{E}$ proliferation
α_e	represents the $\mathcal{E}$ recruitment
$C_{\max}$	represents the maximum C
r_c	is the C growth
γ_e	represents the $\mathcal{E}$ loss due to $\mathcal{T}$
γ_c	represents the C loss due to $\mathcal{E}$

along with initial conditions

$$\mathcal{T}(0) = \mathcal{T}_0, \quad \mathcal{E}(0) = \mathcal{E}_0, \quad C(0) = C_0, \tag{2}$$

where $\mathcal{T}$ represents the native T-cells, $\mathcal{E}$ represents the effector T-cells particular with CML, and C represents the CML cancer cells. Description of the nomenclatures is given in Table 1.

Recently the significant applications of FFD operators have been found. Because the mentioned operators can describe many real-world process with irregular or complex geometry with more excellent ways. The said area has been found very fruitful in studying epidemiological as well as other chronic disease models in terms of mathematical concepts [56,57]. Therefore, our aim of this study is to establish sufficient conditions for the existence theory as well as numerical solutions for the proposed model given in Eq. (1) for three different FFD operators. The three different FFD operators contain power law, exponential and Mittag–Leffler-type kernels. Each and every operator has its own merits properties, which have been discussed in detail in the study by Khan and Atangana [58]. Therefore, we first consider the model given in Eq. (1) under the FFD operator with power-law kernel as

$$\begin{cases} {}^{PFFD}_{0}\mathcal{D}_t^{\varrho,\beta}(\mathcal{T}(t)) = s_n - d_n\mathcal{T} - k_n\mathcal{T}\left(\dfrac{C}{C+\eta}\right), \\ {}^{PFFD}_{0}\mathcal{D}_t^{\varrho,\beta}(\mathcal{E}(t)) = \varrho_n k_n\mathcal{T}\left(\dfrac{C}{C+\eta}\right) + \alpha_e\mathcal{E}\left(\dfrac{C}{C+\eta}\right) - d_e\mathcal{E} \\ \qquad\qquad - \gamma_e C\mathcal{E}, \\ {}^{PFFD}_{0}\mathcal{D}_t^{\varrho,\beta}(C(t)) = r_c C\ln\left(\dfrac{C_{\max}}{C}\right) - d_c C - \gamma_c C\mathcal{E}. \end{cases} \tag{3}$$

Furthermore, since the FFD operators have exponential and Mittag–Leffler kernels also attracted proper attentions from researchers in the past few years. These operators exhibit some more keen features to use in the analysis of disease models. Therefore, we also consider our proposed Model (1) under the FFD operator with exponential kernel as

$$\begin{cases} {}^{EFFD}_{0}\mathcal{D}_t^{\varrho,\beta}(\mathcal{T}(t)) = s_n - d_n\mathcal{T} - k_n\mathcal{T}\left(\dfrac{C}{C+\eta}\right), \\ {}^{EFFD}_{0}\mathcal{D}_t^{\varrho,\beta}(\mathcal{E}(t)) = \varrho_n k_n\mathcal{T}\left(\dfrac{C}{C+\eta}\right) + \alpha_e\mathcal{E}\left(\dfrac{C}{C+\eta}\right) - d_e\mathcal{E} \\ \qquad\qquad - \gamma_e C\mathcal{E}, \\ {}^{EFFD}_{0}\mathcal{D}_t^{\varrho,\beta}(C(t)) = r_c C\ln\left(\dfrac{C_{\max}}{C}\right) - d_c C - \gamma_c C\mathcal{E}. \end{cases} \tag{4}$$

The FFD operator with exponential kernel has been generalized to FFD operator with Mittag–Leffler kernel. Therefore, we also undertake our proposed Model (1) under the Mittag–Leffler-type kernel as

$$\begin{cases} {}^{MFFD}_{0}\mathcal{D}_t^{\varrho,\beta}(\mathcal{T}(t)) = s_n - d_n\mathcal{T} - k_n\mathcal{T}\left(\dfrac{C}{C+\eta}\right), \\ {}^{MFFD}_{0}\mathcal{D}_t^{\varrho,\beta}(\mathcal{E}(t)) = \varrho_n k_n\mathcal{T}\left(\dfrac{C}{C+\eta}\right) + \alpha_e\mathcal{E}\left(\dfrac{C}{C+\eta}\right) - d_e\mathcal{E} \\ \qquad\qquad - \gamma_e C\mathcal{E}, \\ {}^{MFFD}_{0}\mathcal{D}_t^{\varrho,\beta}(C(t)) = r_c C\ln\left(\dfrac{C_{\max}}{C}\right) - d_c C - \gamma_c C\mathcal{E}. \end{cases} \tag{5}$$

We use fixed point theory to establish the local existence and uniqueness for the aforementioned systems of FFD operators as (3)–(5), respectively. Furthermore, using the Adams–Bashforth numerical method [59], we establish numerical schemes for the three considered FFD operators systems. Various numerical results are presented graphically for the proposed model. Also, for the existence theory, we use a fixed point theory from Istratescu [60].

Our manuscript is arranged as follows: detailed introduction is given in Section 1. Preliminaries are given in Section 2. Our first part of main results is given in Section 3. Numerical schemes have developed in Section 4. In addition, numerical simulations are performed in Section 5. Finally, discussion and conclusion are given in Section 6.

2 Preliminaries

Consider that $\mathcal{H}(t)$ be continuous and also fractal differentiable on the interval (m, n). Let $0 < \varrho, \beta \le 1$, where ϱ, and β stand for the fractional orders and fractal dimension, respectively. Here, FFI represents the fractal-fractional integral.

Definition 2.1. [58] The Riemann–Liouville (R-L) FFD operator with power-law-type kernel of $\mathcal{H}(t)$ is defined by

$$ {}^{PFFD}_{0}\mathcal{D}_{t}^{\varrho,\beta}(\mathcal{H}(t)) = \frac{1}{\Gamma(m-\varrho)}\frac{\mathrm{d}}{\mathrm{d}t^{\beta}}\int_{0}^{t}(t-\xi)^{m-\varrho-1}\mathcal{H}(\xi)\mathrm{d}\xi, $$

where $\frac{\mathrm{d}}{\mathrm{d}\xi^{\beta}}\mathcal{H}(\xi) = \lim_{t\to\xi}\frac{\mathcal{H}(t)-\mathcal{H}(\xi)}{t^{\beta}-\xi^{\beta}}$.

Definition 2.2. [58] The FFD operator of $\mathcal{H}(t)$ with exponential kernel is defined as

$$ {}^{EFFD}_{0}\mathcal{D}_{t}^{\varrho,\beta}(\mathcal{H}(t)) = \frac{\mathcal{M}(\varrho)}{1-\varrho}\frac{\mathrm{d}}{\mathrm{d}t^{\beta}}\int_{0}^{t}\exp\left[-\frac{\varrho}{1-\varrho}(t-\xi)\right]\mathcal{H}(\xi)\mathrm{d}\xi, $$

where $\mathcal{M}(\varrho) = (1-\varrho) + \frac{\varrho}{\Gamma(\varrho)}$.

Definition 2.3. [58] The FFD operator with Mittag–Leffler kernel given by of $\mathcal{H}(t)$ is presented by

$$ {}^{MFFD}_{0}\mathcal{D}_{t}^{\varrho,\beta}(\mathcal{H}(t)) = \frac{\mathcal{M}(\varrho)}{1-\varrho}\frac{\mathrm{d}}{\mathrm{d}t^{\beta}}\int_{0}^{t}E_{\varrho}\left[-\frac{\varrho}{1-\varrho}(t-\xi)^{\varrho}\right]\mathcal{H}(\xi)\mathrm{d}\xi, $$

where $\mathcal{M}(\varrho) = 1-\varrho+\frac{\varrho}{\Gamma(\varrho)}$.

Definition 2.4. [58] The FFI of $\mathcal{H}(t)$ in power-law case is given by

$$ {}^{PFFI}_{0}\mathcal{I}_{t}^{\varrho,\beta}\mathcal{H}(t) = \frac{\beta}{\Gamma(\varrho)}\int_{0}^{t}(t-\xi)^{\varrho-1}\xi^{\beta-1}\mathcal{H}(\xi)\mathrm{d}\xi. $$

Definition 2.5. [58] The FFI of $\mathcal{H}(t)$ with exponential decay type kernel is given by

$$ {}^{EFFI}_{0}\mathcal{I}_{t}^{\varrho,\beta}\mathcal{H}(t) = \frac{\beta(1-\varrho)t^{\beta-1}\mathcal{H}(t)}{\mathcal{M}(\varrho)} + \frac{\varrho\beta}{\mathcal{M}(\varrho)}\int_{0}^{t}\xi^{\beta-1}\mathcal{H}(\xi)\mathrm{d}\xi. $$

Definition 2.6. [58] The FFI of $\mathcal{H}(t)$ with Mittag–Leffler-type kernel is

$$ {}^{MFFI}_{0}\mathcal{I}_{t}^{\varrho,\beta}\mathcal{H}(t) = \frac{(1-\varrho)\beta t^{\beta-1}\mathcal{H}(t)}{\mathcal{M}(\varrho)} + \frac{\varrho\beta}{\mathcal{M}(\varrho)}\int_{0}^{t}\xi^{\varrho-1}(t-\xi)^{\beta-1}\mathcal{H}(\xi)\mathrm{d}\xi. $$

3 Main work

We compute the equilibria points of Model (3). If we put left sides of Model (3) equal to zero, then one has $\widetilde{\mathcal{T}} = \frac{s_n}{d_n}$, and from the second equation of Eq. (3), one has $\widetilde{\mathcal{E}} = 0$. In addition, there does not exist any other equilibria for which $\widetilde{C} = 0$. Hence, $E^0 = (\widetilde{\mathcal{T}}, \widetilde{\mathcal{E}}, \widetilde{C}) = \left(\frac{s_n}{d_n}, 0, 0\right)$ represents the healthy (trivial) equilibrium solution of System (3). Furthermore, it has been proved in the study by Moore and Li [55] that the equilibrium point E^0 is asymptotically stable.

Theorem 3.1. *The trivial equilibrium point E^0 is locally asymptotically stable.*

Proof. The Jacobian matrix of Model (3) at $E^0 = \left(\frac{s_n}{d_n}, 0, 0\right)$ is given by

$$ \mathbb{J}(E^0) = \begin{pmatrix} -\frac{s_n}{d_n} & 0 & \frac{k_n}{\gamma_C} \\ 0 & -\frac{\mathrm{d}_e}{d_n} & \frac{\eta d_n^2}{\alpha_n k_n s_n} \\ 0 & 0 & -\frac{(\gamma_C + d_C)}{d_n} \end{pmatrix}. $$

The eigen values of $\mathbb{J}(E^0)$ are given by $\lambda_1 = -\frac{s_n}{d_n}$, $\lambda_2 = -\frac{\mathrm{d}_e}{d_n}$, and $\lambda_3 = -\frac{(\gamma_C + d_C)}{d_n}$. We see that the real parts of all eigen values are negative. Therefore, the equilibrium point E^0 is locally asymptotically stable. □

Remark 3.2. Moreover, any other non-trivial equilibria are denoted by $E^* = (\widetilde{\mathcal{T}}^*, \widetilde{\mathcal{E}}^*, \widetilde{C}^*)$. In the third equation of the proposed model, the logarithmic function of C is involved. Therefore, third equation increases as C increases. Hence, for the term to be zero in third equation of the proposed model, C must be negative. Thus, the expression in the third equation decreases if $C > 0$. Hence, there exists a unique value of C for which the third equation of Model (3) becomes zero. Thus, we conclude that there exists at most one equilibrium point E^*, which occurs only if

$$ d_n > \gamma_C \ln\left(\frac{\gamma_C C_{\max}}{d_n}\right). $$

Hence, this equilibrium must have three nonnegative populations for it to have any physical significance. Keeping in mind this discussion, as all parameters of Model (3) are positive, hence from the first equation of Model (3), $\mathcal{T}_0 > 0, \mathcal{E}_0 > 0, C_0 > 0$, the solution $\mathcal{T}(t) > 0, \mathcal{E}(t) > 0$, and $C(t) > 0$, for every $t \in [0, b]$, $b < \infty$. Hence, we conclude that if

$$ d_n < \gamma_C \ln\left(\frac{\gamma_C C_{\max}}{d_n}\right) $$

holds, then both E^0 and E^* are globally asymptotically stable.

We will explore the existence and the uniqueness of solution of the suggested model's solution under the FFD with all the three different kernels using fixed point theory

in this part. For other types of operators, one can easily derive the existence results. We will use the given theorem for the existence and uniqueness of solution. Here, $X = C[0, T]$ is the Banach space, then $\mathbf{Z} = X \times X \times X$ is also Banach space with norm defined by

$$\|\Psi\|_\infty = \sup_{t\in[0,T]} |\Psi(t)|.$$

Theorem 3.3. [60] *Let O be a contraction operator on a Banach space say $\mathbf{Z}$, then O has a unique fixed point.*

Let us write System (3) as follows using $\Phi = (\mathcal{T}, \mathcal{E}, C)$:

$$\begin{aligned} {}^{PFFD}_{0}\mathcal{D}_t^{\varrho,\beta}[\Phi(t)] &= \mathscr{F}(t, \Phi(t)),\\ \Phi(0) &= \Phi_0 \end{aligned} \tag{6}$$

where

$$\Phi(t) = \begin{cases} \mathcal{T}(t),\\ \mathcal{E}(t),\\ C(t), \end{cases}$$

and

$$\mathscr{F}(t, \Phi(t)) = \begin{cases} \mathcal{H}_1(t, \mathcal{T}, \mathcal{E}, C) = s_n - d_n\mathcal{T} - k_n\mathcal{T}\left(\dfrac{C}{C+\eta}\right),\\ \mathcal{H}_2(t, \mathcal{T}, \mathcal{E}, C) = \varrho_n k_n\mathcal{T}\left(\dfrac{C}{C+\eta}\right) + \alpha_e\mathcal{E}\left(\dfrac{C}{C+\eta}\right)\\ \qquad\qquad - d_e\mathcal{E} - \gamma_e C\mathcal{E},\\ \mathcal{H}_3(t, \mathcal{T}, \mathcal{E}, C) = r_c C\ln\left(\dfrac{C_{\max}}{C}\right) - d_c C - \gamma_c C\mathcal{E}. \end{cases}$$

Replacing the R-L derivative of fractional order ϱ (6) by the Caputo to include initial condition, we obtain the equivalent integral form as follows:

$$\Phi(t) = \Phi_0 + \frac{\beta}{\Gamma(\varrho)}\int_0^t \xi^{\beta-1}(t-\xi)^{\varrho-1}\mathscr{F}(\xi, \Phi(\xi))\mathrm{d}\xi. \tag{7}$$

Since $(\mathcal{T}, \mathcal{E}, C)$ is bounded, we further described assumptions as:

(A1) $\mathscr{F}(t, \Phi(t))$ is continuous and bounded.

(A2) There is a constant $M_{\mathscr{F}} > 0$, we have for $\Phi, \bar{\Phi} \in \mathbf{Z}$,

$$|\mathscr{F}(t, \Phi) - \mathscr{F}(t, \bar{\Phi})| \le M_{\mathscr{F}}|\Phi - \bar{\Phi}|.$$

Theorem 3.4. *The proposed Model* (3) *has a unique solution if* $\mathcal{K} = \frac{\beta M_{\mathscr{F}}\mathbf{B}(\beta,\varrho)}{\Gamma(\varrho)} < 1$, *where* $\mathbf{B}(\beta, \varrho)$ *is the beta function defined by*

$$\mathbf{B}(\beta, \varrho) = \frac{\Gamma(\beta)\Gamma(\varrho)}{\Gamma(\beta+\varrho)}.$$

Proof. Let us define the operator $O : \mathbf{Z} \to \mathbf{Z}$ by

$$\begin{aligned} O\Phi(t) = \Phi_0 + \frac{\varrho}{\Gamma(\beta)}\int_0^t \xi^{\beta-1}(t-\xi)^{\varrho-1}[\mathscr{F}(\xi, \Phi(\xi))\\ - \mathscr{F}(\xi, \bar{\Phi}(\xi))]\mathrm{d}\xi. \end{aligned} \tag{8}$$

Let $\Phi, \bar{\Phi} \in \mathbf{Z}$, using the assumption A_2, we have

$$\begin{aligned} &\|O\Phi - O\bar{\Phi}\|_\infty\\ &= \sup_{t\in[0,T]}\left|\frac{\beta}{\Gamma(\varrho)}\int_0^t \xi^{\beta-1}(t-\xi)^{\varrho-1}\mathscr{F}(\xi, \Phi(\xi))\mathrm{d}\xi\right|\\ &\le \sup_{t\in[0,T]}\frac{\beta}{\Gamma(\varrho)}\int_0^t \xi^{\beta-1}(t-\xi)^{\varrho-1}|\mathscr{F}(\xi, \Phi(\xi)) - \mathscr{F}(\xi, \bar{\Phi}(\xi))|\mathrm{d}\xi\\ &\le \sup_{t\in[0,T]}\frac{\beta}{\Gamma(\varrho)}\int_0^t \xi^{\beta-1}(t-\xi)^{\varrho-1}M_{\mathscr{F}}|\Phi(\xi) - \bar{\Phi}(\xi)|\mathrm{d}\xi\\ &\le \frac{\beta M_{\mathscr{F}}\|\Phi - \bar{\Phi}\|_\infty}{\Gamma(\varrho)}\int_0^T \xi^{\beta-1}(T-\xi)^{\varrho-1}\mathrm{d}\xi\\ &= \mathcal{K}\|\Phi - \bar{\Phi}\|_\infty, \end{aligned}$$

where

$$\int_0^T \xi^{\beta-1}(T-\xi)^{\varrho-1}\mathrm{d}\xi = T^{\varrho+\beta-1}\mathbf{B}(\beta, \varrho).$$

Hence, one has

$$\|O\Phi - O\bar{\Phi}\|_\infty \le \mathcal{K}\|\Phi - \bar{\Phi}\|_\infty,$$

which shows that O satisfies the Banach contraction theorem. Thus, Problem (3) has a unique solution. □

By Definition 2.3, we have

$${}^{MFFD}_{0}\mathcal{D}_t^{\varrho,\beta}[\Phi(t)] = \frac{\mathcal{M}(\varrho)}{1-\varrho}\frac{\mathrm{d}}{\mathrm{d}t^\beta}\int_0^t \mathscr{F}(\xi, \Phi(\xi))E_\varrho \times\left(-\frac{\varrho}{1-\varrho}(t-\xi)^\varrho\right)\mathrm{d}\xi.$$

Since the integral is differentiable, we achieve

$${}^{MFFD}_{0}\mathcal{D}_t^{\varrho}[\Phi(t)] = \frac{1}{\beta t^{\beta-1}}\frac{\mathcal{M}(\varrho)}{1-\varrho}\frac{\mathrm{d}}{\mathrm{d}t} \times\int_0^t \mathscr{F}(\xi, \Phi(\xi))E_\varrho\left(-\frac{\varrho}{1-\varrho}(t-\xi)^\varrho\right)\mathrm{d}\xi.$$

Eq. (7) becomes

$$\begin{aligned} &\frac{\mathcal{M}(\varrho)}{1-\varrho}\frac{\mathrm{d}}{\mathrm{d}t}\int_0^t \mathscr{F}(\xi, \Phi(\xi))E_\varrho\\ &\times\left(-\frac{\varrho}{1-\varrho}(t-\xi)^\varrho\right)\mathrm{d}\xi = \beta t^{\beta-1}\mathscr{F}(t, \Phi(t)). \end{aligned} \tag{9}$$

Replacing the R-L derivative of fractional order ϱ (9) by the Caputo to include initial condition, we obtain the equivalent integral form as follows:

$$\Phi(t) = \Phi(0) + \frac{1-\varrho}{\mathcal{M}(\varrho)}\beta t^{\beta-1}\mathscr{F}(t,\Phi(t)) + \frac{\varrho\beta}{\mathcal{M}(\varrho)\Gamma(\varrho)}\int_0^t (t-\xi)^{\varrho-1}\mathscr{F}(\xi,\Phi(\xi))\xi^{\beta-1}\mathrm{d}\xi. \tag{10}$$

Theorem 3.5. *Model* (4) *has a unique solution if* $\mathcal{K}_1 = \left[\frac{\beta T^{\beta-1}(1-\varrho)}{\mathcal{M}(\varrho)} + \frac{\varrho\beta T^{\varrho+\beta-1}\mathbf{B}(\varrho,\beta)}{\mathcal{M}(\varrho)\Gamma(\varrho)}\right]M_{\mathscr{F}} < 1$ *holds.*

Proof. Let us define the operator by

$$O\Phi(t) = \Phi(0) + \frac{1-\varrho}{\mathcal{M}(\varrho)}\beta t^{\beta-1}\mathscr{F}(t,\Phi(t)) + \frac{\varrho\beta}{\mathcal{M}(\varrho)\Gamma(\varrho)}\int_0^t (t-\xi)^{\varrho-1}\mathscr{F}(\xi,\Phi(\xi))\xi^{\beta-1}\mathrm{d}\xi. \tag{11}$$

Let $\Psi, \bar{\Psi} \in \mathbf{Z}$, using assumption A_2, we have

$$\begin{aligned}
\|O\Phi - O\bar{\Phi}\|_\infty &\le \sup_{t\in[0,T]}\left|\frac{1-\varrho}{\mathcal{M}(\varrho)}\beta t^{\beta-1}\mathscr{F}(t,\Phi(t)) - \frac{1-\varrho}{\mathcal{M}(\varrho)}\beta t^{\beta-1}\mathscr{F}(t,\bar{\Phi}(t))\right| \\
&\quad + \sup_{t\in[0,T]}\left|\frac{\varrho\beta}{\mathcal{M}(\varrho)\Gamma(\varrho)}\int_0^t \xi^{\beta-1}(t-\xi)^{\varrho-1}\mathscr{F}(\xi,\Phi(\xi))\mathrm{d}\xi - \frac{\varrho\beta}{\mathcal{M}(\varrho)\Gamma(\varrho)}\int_0^t \xi^{\beta-1}(t-\xi)^{\varrho-1}\mathscr{F}(\xi,\bar{\Phi}(\xi))\mathrm{d}\xi\right| \\
&\le \frac{M_{\mathscr{F}}(1-\varrho)}{\mathcal{M}(\varrho)}\beta T^{\beta-1}\|\Phi-\bar{\Phi}\|_\infty + \frac{\varrho\beta}{\mathcal{M}(\varrho)\Gamma(\varrho)}M_{\mathscr{F}}\|\Phi-\bar{\Phi}\|_\infty\int_0^T \xi^{\beta-1}(T-\xi)^{\varrho-1}\mathrm{d}\xi \\
&= \left[\frac{\beta T^{\beta-1}(1-\varrho)}{\mathcal{M}(\varrho)} + \frac{\varrho\beta\mathbf{B}(\varrho,\beta)T^{\varrho+\beta-1}}{\mathcal{M}(\varrho)\Gamma(\varrho)}\right]M_{\mathscr{F}}\|\Phi-\bar{\Phi}\|_\infty \\
&= \mathcal{K}_1\|\Phi-\bar{\Phi}\|_\infty,
\end{aligned}$$

which implies that

$$\|O\Phi - O\bar{\Phi}\|_\infty \le \mathcal{K}_1\|\Phi-\bar{\Phi}\|_\infty,$$

so O is a contraction and has a unique fixed point. Therefore, Model (5) has a unique solution. □

Remark 3.6. The same procedure of Theorem 3.5 can be repeated for Model (4) to show the existence of unique solution.

4 Numerical schemes

We will use the Lagrange piecewise interpolation to generate numerical schemes for the proposed models under three different kinds of FFD operators. In this section, we discuss the following three cases.

4.1 Numerical scheme for Model (3)

Now, we will derive the numerical scheme of Model (3) FFD operator with power-law kernel. From System (3), we have

$$\begin{cases}
{}^{\mathcal{RL}}\mathcal{D}^{\varrho}_{0,t}(\mathcal{T}(t)) = \beta t^{\beta-1}\left[s_n - d_n\mathcal{T} - k_n\mathcal{T}\left(\frac{C}{C+\eta}\right)\right], \\
{}^{\mathcal{RL}}\mathcal{D}^{\varrho}_{0,t}(\mathcal{E}(t)) = \beta t^{\beta-1}\left[\varrho_n k_n\mathcal{T}\left(\frac{C}{C+\eta}\right) + \alpha_e\mathcal{E}\left(\frac{C}{C+\eta}\right) - d_e\mathcal{E} - \gamma_e C\mathcal{E}\right], \\
{}^{\mathcal{RL}}\mathcal{D}^{\varrho}_{0,t}(C(t)) = \beta t^{\beta-1}\left[r_c C\ln\left(\frac{C_{\max}}{C}\right) - d_c C - \gamma_c C\mathcal{E}\right].
\end{cases} \tag{12}$$

Replacing the R-L derivative of fractional order ϱ (12) by the Caputo to include initial condition, we obtain the equivalent integral system as follows:

$$\begin{cases}
\mathcal{T}(t) = \mathcal{T}(0) + \frac{\beta}{\Gamma(\varrho)}\int_0^t \xi^{\beta-1}(t-\xi)^{\varrho-1}\mathcal{H}_1(\xi,\mathcal{T},\mathcal{E},C)\mathrm{d}\xi, \\
\mathcal{E}(t) = \mathcal{E}(0) + \frac{\beta}{\Gamma(\varrho)}\int_0^t \xi^{\beta-1}(t-\xi)^{\varrho-1}\mathcal{H}_2(\xi,\mathcal{T},\mathcal{E},C)\mathrm{d}\xi, \\
C(t) = C(0) + \frac{\beta}{\Gamma(\varrho)}\int_0^t \xi^{\beta-1}(t-\xi)^{\varrho-1}\mathcal{H}_3(\xi,\mathcal{T},\mathcal{E},C)\mathrm{d}\xi,
\end{cases} \tag{13}$$

where

$$\begin{cases}
\mathcal{H}_1(\xi,\mathcal{T},\mathcal{E},C) = s_n - d_n\mathcal{T} - k_n\mathcal{T}\left(\frac{C}{C+\eta}\right), \\
\mathcal{H}_2(\xi,\mathcal{T},\mathcal{E},C) = \varrho_n k_n\mathcal{T}\left(\frac{C}{C+\eta}\right) + \alpha_e\mathcal{E}\left(\frac{C}{C+\eta}\right) - d_e\mathcal{E} - \gamma_e C\mathcal{E}, \\
\mathcal{H}_3(\xi,\mathcal{T},\mathcal{E},C) = r_c C\ln\left(\frac{C_{\max}}{C}\right) - d_c C - \gamma_c C\mathcal{E}.
\end{cases} \tag{14}$$

Here, we derive the numerical algorithm of the aforementioned system at $t = t_{n+1}$. So, Model (13) becomes

$$\begin{cases} \mathcal{T}^{n+1} = \mathcal{T}^0 \\ \qquad + \dfrac{\beta}{\Gamma(\varrho)} \displaystyle\int_0^{t_{n+1}} \xi^{\beta-1}(t_{n+1}-\xi)^{\varrho-1}\mathcal{H}_1(\xi,\mathcal{T},\mathcal{E},C)\mathrm{d}\xi, \\ \mathcal{E}^{n+1} = \mathcal{E}^0 \\ \qquad + \dfrac{\beta}{\Gamma(\varrho)} \displaystyle\int_0^{t_{n+1}} \xi^{\beta-1}(t_{n+1}-\xi)^{\varrho-1}\mathcal{H}_2(\xi,\mathcal{T},\mathcal{E},C)\mathrm{d}\xi, \\ C^{n+1} = C^0 + \dfrac{\beta}{\Gamma(\varrho)} \displaystyle\int_0^{t_{n+1}} \xi^{\beta-1}(t_{n+1}-\xi)^{\varrho-1}\mathcal{H}_3(\xi,\mathcal{T},\mathcal{E},C)\mathrm{d}\xi. \end{cases} \tag{15}$$

Then, the approximation of the aforementioned system is given as follows:

$$\begin{cases} \mathcal{T}^{n+1} = \mathcal{T}^0 \\ \qquad + \dfrac{\beta}{\Gamma(\varrho)} \displaystyle\sum_{\Omega=0}^{n} \int_0^{t_{\Omega+1}} \xi^{\beta-1}(t_{n+1}-\xi)^{\varrho-1}\mathcal{H}_1(\xi,\mathcal{T},\mathcal{E},C)\mathrm{d}\xi, \\ \mathcal{E}^{n+1} = \mathcal{E}^0 \\ \qquad + \dfrac{\beta}{\Gamma(\varrho)} \displaystyle\sum_{\Omega=0}^{n} \int_0^{t_{\Omega+1}} \xi^{\beta-1}(t_{n+1}-\xi)^{\varrho-1}\mathcal{H}_2(\xi,\mathcal{T},\mathcal{E},C)\mathrm{d}\xi, \\ C^{n+1} = C^0 + \dfrac{\beta}{\Gamma(\varrho)} \displaystyle\sum_{\Omega=0}^{n} \int_0^{t_{\Omega+1}} \xi^{\beta-1}(t_{n+1}-\xi)^{\varrho-1}\mathcal{H}_3(\xi,\mathcal{T},\mathcal{E},C)\mathrm{d}\xi. \end{cases} \tag{16}$$

We approximate the function $\xi^{\beta-1}\mathcal{H}_1(\xi,\mathcal{T},\mathcal{E},C)$ using the Lagrangian piece-wise interpolation (LPI) in $[t_\Omega, t_{\Omega+1}]$ as follows:

$$\begin{cases} \mathscr{P}_\Omega(\xi) = \dfrac{\xi - t_{\Omega-1}}{t_\Omega - t_{\Omega-1}} t_\Omega^{\beta-1}\mathcal{H}_1(t^\Omega,\mathcal{T}^\Omega,\mathcal{E}^\Omega,C^\Omega) \\ \qquad - \dfrac{\xi - t_\Omega}{t_\Omega - t_{\Omega-1}} t_{\Omega-1}^{\beta-1}\mathcal{H}_1(t^{\Omega-1},\mathcal{T}^{\Omega-1},\mathcal{E}^{\Omega-1},C^{\Omega-1}), \\ \mathscr{Q}_\Omega(\xi) = \dfrac{\xi - t_{\Omega-1}}{t_\Omega - t_{\Omega-1}} t_\Omega^{\beta-1}\mathcal{H}_2(t^\Omega,\mathcal{T}^\Omega,\mathcal{E}^\Omega,C^\Omega) \\ \qquad - \dfrac{\xi - t_\Omega}{t_\Omega - t_{\Omega-1}} t_{\Omega-1}^{\beta-1}\mathcal{H}_2(t^{\Omega-1},\mathcal{T}^{\Omega-1},\mathcal{E}^{\Omega-1},C^{\Omega-1}), \\ \mathscr{R}_\Omega(\xi) = \dfrac{\xi - t_{\Omega-1}}{t_\Omega - t_{\Omega-1}} t_\Omega^{\beta-1}\mathcal{H}_3(t^\Omega,\mathcal{T}^\Omega,\mathcal{E}^\Omega,C^\Omega) \\ \qquad - \dfrac{\xi - t_\Omega}{t_\Omega - t_{\Omega-1}} t_{\Omega-1}^{\beta-1}\mathcal{H}_3(t^{\Omega-1},\mathcal{T}^{\Omega-1},\mathcal{E}^{\Omega-1},C^{\Omega-1}). \end{cases} \tag{17}$$

Thus, System (16) becomes

$$\begin{cases} \mathcal{T}^{n+1} = \mathcal{T}^0 + \dfrac{\beta}{\Gamma(\varrho)} \displaystyle\sum_{\Omega=0}^{n} \int_0^{t_{\Omega+1}} \xi^{\beta-1}(t_{n+1}-\xi)^{\varrho-1}\mathscr{P}_\Omega(\xi)\mathrm{d}\xi, \\ \mathcal{E}^{n+1} = \mathcal{E}^0 + \dfrac{\beta}{\Gamma(\varrho)} \displaystyle\sum_{\Omega=0}^{n} \int_0^{t_{\Omega+1}} \xi^{\beta-1}(t_{n+1}-\xi)^{\varrho-1}\mathscr{Q}_\Omega(\xi)\mathrm{d}\xi, \\ C^{n+1} = C^0 + \dfrac{\beta}{\Gamma(\varrho)} \displaystyle\sum_{\Omega=0}^{n} \int_0^{t_{\Omega+1}} \xi^{\beta-1}(t_{n+1}-\xi)^{\varrho-1}\mathscr{R}_\Omega(\xi)\mathrm{d}\xi. \end{cases} \tag{18}$$

Then, we reach

$$\begin{cases} \mathcal{T}^{n+1} = \mathcal{T}^0 + \dfrac{\beta(\Delta t)^\varrho}{\Gamma(\varrho+2)} \displaystyle\sum_{\Omega=0}^{n} [t_{\Omega-1}^{\beta-1}\mathcal{H}_1(t_\Omega,\mathcal{T}^\Omega,\mathcal{E}^\Omega,C^\Omega) \\ \qquad \times ((n+1-\Omega)^\varrho(n-\Omega+2+\varrho) \\ \qquad - (n-\Omega)^\varrho(n-\Omega+2+2\varrho)) \\ \qquad - t_{\Omega-1}^{\beta-1}\mathcal{H}_1(t_{\Omega-1},\mathcal{T}^{\Omega-1},\mathcal{E}^{\Omega-1},C^{\Omega-1}) \\ \qquad \times ((n+1-\Omega)^{\varrho+1} - (n-\Omega)^\varrho(n-\Omega+1 \\ \qquad + \varrho))], \\ \mathcal{E}^{n+1} = \mathcal{E}^0 + \dfrac{\beta(\Delta t)^\varrho}{\Gamma(\varrho+2)} \displaystyle\sum_{\Omega=0}^{n} [t_{\Omega-1}^{\beta-1}\mathcal{H}_2(t_\Omega,\mathcal{T}^\Omega,\mathcal{E}^\Omega,C^\Omega) \\ \qquad \times ((n+1-\Omega)^\varrho(n-\Omega+2+\varrho) \\ \qquad - (n-\Omega)^\varrho(n-\Omega+2+2\varrho)) \\ \qquad - t_{\Omega-1}^{\beta-1}\mathcal{H}_2(t_{\Omega-1},\mathcal{T}^{\Omega-1},\mathcal{E}^{\Omega-1},C^{\Omega-1}) \\ \qquad \times ((n+1-\Omega)^{\varrho+1} - (n-\Omega)^\varrho(n-\Omega+1 \\ \qquad + \varrho))], \\ C^{n+1} = C^0 + \dfrac{\beta(\Delta t)^\varrho}{\Gamma(\varrho+2)} \displaystyle\sum_{\Omega=0}^{n} [t_{\Omega-1}^{\beta-1}\mathcal{H}_3(t_\Omega,\mathcal{T}^\Omega,\mathcal{E}^\Omega,C^\Omega) \\ \qquad \times ((n+1-\Omega)^\varrho(n-\Omega+2+\varrho) \\ \qquad - (n-\Omega)^\varrho(n-\Omega+2+2\varrho)) \\ \qquad - t_{\Omega-1}^{\beta-1}\mathcal{H}_3(t_{\Omega-1},\mathcal{T}^{\Omega-1},\mathcal{E}^{\Omega-1},C^{\Omega-1}) \\ \qquad \times ((n+1-\Omega)^{\varrho+1} - (n-\Omega)^\varrho(n-\Omega+1 \\ \qquad + \varrho))]. \end{cases} \tag{19}$$

4.2 Numerical scheme for Model (4)

Here, we set a numerical scheme for the proposed model under the FFD operator with exponential kernel. Therefore, applying the Caputo–Fabrizio integral to Eq. (4) to obtain the following system of integral equations as follows:

$$\begin{cases} \mathcal{T}(t) = \mathcal{T}(0) + \dfrac{\beta t^{\beta-1}(1-\varrho)}{\mathcal{M}(\varrho)}\mathcal{H}_1(t,\mathcal{T},\mathcal{E},C) \\ \qquad + \dfrac{\varrho\beta}{\mathcal{M}(\varrho)}\displaystyle\int_0^t \xi^{\beta-1}\mathcal{H}_1(t,\mathcal{T},\mathcal{E},C), \\ \mathcal{E}(t) = \mathcal{E}(0) + \dfrac{\beta t^{\beta-1}(1-\varrho)}{\mathcal{M}(\varrho)}\mathcal{H}_2(t,\mathcal{T},\mathcal{E},C) \\ \qquad + \dfrac{\varrho\beta}{\mathcal{M}(\varrho)}\displaystyle\int_0^t \xi^{\beta-1}\mathcal{H}_2(t,\mathcal{T},\mathcal{E},C), \\ C(t) = C(0) + \dfrac{\beta t^{\beta-1}(1-\varrho)}{\mathcal{M}(\varrho)}\mathcal{H}_3(t,\mathcal{T},\mathcal{E},C) \\ \qquad \dfrac{\varrho\beta}{\mathcal{M}(\varrho)}\displaystyle\int_0^t \xi^{\beta-1}\mathcal{H}_3(t,\mathcal{T},\mathcal{E},C). \end{cases} \tag{20}$$

The derivation of the numerical scheme is presented at $t = t_{n+1}$. Thus,

$$\begin{cases} \mathcal{T}^{n+1} = \mathcal{T}^0 + \dfrac{\beta t_n^{\beta-1}(1-\varrho)}{\mathcal{M}(\varrho)}\mathcal{H}_1(t_n,\mathcal{T}^n,\mathcal{E}^n,C^n) \\ \qquad + \dfrac{\varrho\beta}{\mathcal{M}(\varrho)}\displaystyle\int_0^{t_{n+1}} \xi^{\beta-1}\mathcal{H}_1(t,\mathcal{T},\mathcal{E},C)\mathrm{d}\xi, \\ \mathcal{E}^{n+1} = \mathcal{E}^0 + \dfrac{\beta t_n^{\beta-1}(1-\varrho)}{\mathcal{M}(\varrho)}\mathcal{H}_2(t_n,\mathcal{T}^n,\mathcal{E}^n,C^n) \\ \qquad + \dfrac{\varrho\beta}{\mathcal{M}(\varrho)}\displaystyle\int_0^{t_{n+1}} \xi^{\beta-1}\mathcal{H}_2(t,\mathcal{T},\mathcal{E},C)\mathrm{d}\xi, \\ C^{n+1} = C^0 + \dfrac{\beta t_n^{\beta-1}(1-\varrho)}{\mathcal{M}(\varrho)}\mathcal{H}_3(t_n,\mathcal{T}^n,\mathcal{E}^n,C^n) \\ \qquad \dfrac{\varrho\beta}{\mathcal{M}(\varrho)}\displaystyle\int_0^{t_{n+1}} \xi^{\beta-1}\mathcal{H}_3(t,\mathcal{T},\mathcal{E},C)\mathrm{d}\xi. \end{cases} \tag{21}$$

Taking the difference between the consecutive terms, one have

$$\begin{cases} \mathcal{T}^{n+1} = \mathcal{T}^n + \dfrac{\beta t_n^{\beta-1}(1-\varrho)}{\mathcal{M}(\varrho)}\mathcal{H}_1(t_n,\mathcal{T}^n,\mathcal{E}^n,C^n) \\ \qquad - \dfrac{\beta t_{n-1}^{\beta-1}(1-\varrho)}{\mathcal{M}(\varrho)}\mathcal{H}_1(t_{n-1},\mathcal{T}^{n-1},\mathcal{E}^{n-1},C^{n-1}) \\ \qquad + \dfrac{\varrho\beta}{\mathcal{M}(\varrho)}\displaystyle\int_{t_n}^{t_{n+1}} \xi^{\beta-1}\mathcal{H}_1(t,\mathcal{T},\mathcal{E},C)\mathrm{d}\xi, \\ \mathcal{E}^{n+1} = \mathcal{E}^n + \dfrac{\beta t_n^{\beta-1}(1-\varrho)}{\mathcal{M}(\varrho)}\mathcal{H}_2(t_n,\mathcal{T}^n,\mathcal{E}^n,C^n) \\ \qquad - \dfrac{\beta t_{n-1}^{\beta-1}(1-\varrho)}{\mathcal{M}(\varrho)}\mathcal{H}_2(t_{n-1},\mathcal{T}^{n-1},\mathcal{E}^{n-1},C^{n-1}) \\ \qquad + \dfrac{\varrho\beta}{\mathcal{M}(\varrho)}\displaystyle\int_{t_n}^{t_{n+1}} \xi^{\beta-1}\mathcal{H}_2(t,\mathcal{T},\mathcal{E},C)\mathrm{d}\xi, \\ C^{n+1} = C^n + \dfrac{\beta t_n^{\beta-1}(1-\varrho)}{\mathcal{M}(\varrho)}\mathcal{H}_3(t_n,\mathcal{T}^n,\mathcal{E}^n,C^n) \\ \qquad - \dfrac{\beta t_{n-1}^{\beta-1}(1-\varrho)}{\mathcal{M}(\varrho)}\mathcal{H}_3(t_{n-1},\mathcal{T}^{n-1},\mathcal{E}^{n-1},C^{n-1}) \\ \qquad + \dfrac{\varrho\beta}{\mathcal{M}(\varrho)}\displaystyle\int_{t_n}^{t_{n+1}} \xi^{\beta-1}\mathcal{H}_3(t,\mathcal{T},\mathcal{E},C)\mathrm{d}\xi. \end{cases} \tag{22}$$

Now, by LPI, we have

$$\begin{cases} \mathcal{T}^{n+1} = \mathcal{T}^n + \dfrac{\beta t_n^{\beta-1}(1-\varrho)}{\mathcal{M}(\varrho)}\mathcal{H}_1(t_n,\mathcal{T}^n,\mathcal{E}^n,C^n) \\ \qquad - \dfrac{\beta t_{n-1}^{\beta-1}(1-\varrho)}{\mathcal{M}(\varrho)}\mathcal{H}_1(t_{n-1},\mathcal{T}^{n-1},\mathcal{E}^{n-1},C^{n-1}) + \dfrac{\varrho\beta}{\mathcal{M}(\varrho)} \\ \qquad \times \left[\dfrac{3}{2}(\Delta t)t_n^{\beta-1}\mathcal{H}_1(t_n,\mathcal{T}^n,\mathcal{E}^n,C^n)\right. \\ \qquad \left. - \dfrac{\Delta t}{2}t_{n-1}^{\beta-1}\mathcal{H}_1(t_{n-1},\mathcal{T}^{n-1},\mathcal{E}^{n-1},C^{n-1})\right], \\ \mathcal{E}^{n+1} = \mathcal{E}^n + \dfrac{\beta t_n^{\beta-1}(1-\varrho)}{\mathcal{M}(\varrho)}\mathcal{H}_2(t_n,\mathcal{T}^n,\mathcal{E}^n,C^n) \\ \qquad - \dfrac{\beta t_{n-1}^{\beta-1}(1-\varrho)}{\mathcal{M}(\varrho)}\mathcal{H}_2(t_{n-1},\mathcal{T}^{n-1},\mathcal{E}^{n-1},C^{n-1}) + \dfrac{\varrho\beta}{\mathcal{M}(\varrho)} \\ \qquad \times \left[\dfrac{3}{2}(\Delta t)t_n^{\beta-1}\mathcal{H}_2(t_n,\mathcal{T}^n,\mathcal{E}^n,C^n)\right. \\ \qquad \left. - \dfrac{\Delta t}{2}t_{n-1}^{\beta-1}\mathcal{H}_1(t_{n-1},\mathcal{T}^{n-1},\mathcal{E}^{n-1},C^{n-1})\right], \\ C^{n+1} = C^n + \dfrac{\beta t_n^{\beta-1}(1-\varrho)}{\mathcal{M}(\varrho)}\mathcal{H}_2(t_n,\mathcal{T}^n,\mathcal{E}^n,C^n) \\ \qquad - \dfrac{\beta t_{n-1}^{\beta-1}(1-\varrho)}{\mathcal{M}(\varrho)}\mathcal{H}_2(t_{n-1},\mathcal{T}^{n-1},\mathcal{E}^{n-1},C^{n-1}) + \dfrac{\varrho\beta}{\mathcal{M}(\varrho)} \\ \qquad \times \left[\dfrac{3}{2}(\Delta t)t_n^{\beta-1}\mathcal{H}_2(t_n,\mathcal{T}^n,\mathcal{E}^n,C^n)\right. \\ \qquad \left. - \dfrac{\Delta t}{2}t_{n-1}^{\beta-1}\mathcal{H}_1(t_{n-1},\mathcal{T}^{n-1},\mathcal{E}^{n-1},C^{n-1})\right]. \end{cases} \tag{23}$$

4.3 Numerical scheme for Model (5)

We apply FFI with Mittag–Leffler kernel to (5) to convert the proposed model into the equivalent integral system as

$$\begin{cases} \mathcal{T}(t) = \mathcal{T}(0) + \dfrac{\beta t^{\beta-1}(1-\varrho)}{\mathcal{M}(\varrho)}\mathcal{H}_1(t,\mathcal{T},\mathcal{E},C) \\ \qquad + \dfrac{\varrho\beta}{\mathcal{M}(\varrho)\Gamma(\varrho)}\displaystyle\int_0^t \xi^{\beta-1}(t-\xi)^{\varrho-1}\mathcal{H}_1(\xi,\mathcal{T},\mathcal{E},C)\mathrm{d}\xi, \\ \mathcal{E}(t) = \mathcal{E}(0) + \dfrac{\beta t^{\beta-1}(1-\varrho)}{\mathcal{M}(\varrho)}\mathcal{H}_2(t,\mathcal{T},\mathcal{E},C) \\ \qquad + \dfrac{\varrho\beta}{\mathcal{M}(\varrho)\Gamma(\varrho)}\displaystyle\int_0^t \xi^{\beta-1}(t-\xi)^{\varrho-1}\mathcal{H}_2(\xi,\mathcal{T},\mathcal{E},C)\mathrm{d}\xi, \\ C(t) = C(0) + \dfrac{\beta t^{\beta-1}(1-\varrho)}{\mathcal{M}(\varrho)}\mathcal{H}_3(t,\mathcal{T},\mathcal{E},C) \\ \qquad + \dfrac{\varrho\beta}{\mathcal{M}(\varrho)\Gamma(\varrho)}\displaystyle\int_0^t \xi^{\beta-1}(t-\xi)^{\varrho-1}\mathcal{H}_3(\xi,\mathcal{T},\mathcal{E},C)\mathrm{d}\xi. \end{cases}$$

At $t = t_{n+1}$, we have

$$\begin{cases} \mathcal{T}^{n+1} = \mathcal{T}^0 + \dfrac{\beta t_n^{\beta-1}(1-\varrho)}{\mathcal{M}(\varrho)}\mathcal{H}_1(t_n, \mathcal{T}^n, \mathcal{E}^n, C^n) \\ \quad + \dfrac{\varrho\beta}{\mathcal{M}(\varrho)\Gamma(\varrho)}\displaystyle\int_0^{t_{n+1}} \xi^{\beta-1}(t_{n+1}-\xi)^{\varrho-1} \\ \quad \times \mathcal{H}_1(\xi, \mathcal{T}, \mathcal{E}, C)\mathrm{d}\xi, \\ \mathcal{E}^{n+1} = \mathcal{E}^0 + \dfrac{\beta t_n^{\beta-1}(1-\varrho)}{\mathcal{M}(\varrho)}\mathcal{H}_2(t_n, \mathcal{T}^n, \mathcal{E}^n, C^n) \\ \quad + \dfrac{\varrho\beta}{\mathcal{M}(\varrho)\Gamma(\varrho)}\displaystyle\int_0^{t_{n+1}} \xi^{\beta-1}(t_{n+1}-\xi)^{\varrho-1} \\ \quad \times \mathcal{H}_2(\xi, \mathcal{T}, \mathcal{E}, C)\mathrm{d}\xi, \\ C^{n+1} = C^0 + \dfrac{\beta t_n^{\beta-1}(1-\varrho)}{\mathcal{M}(\varrho)}\mathcal{H}_2(t_n, \mathcal{T}^n, \mathcal{E}^n, C^n) \\ \quad + \dfrac{\varrho\beta}{\mathcal{M}(\varrho)\Gamma(\varrho)}\displaystyle\int_0^{t_{n+1}} \xi^{\beta-1}(t_{n+1}-\xi)^{\varrho-1} \\ \quad \times \mathcal{H}_2(\xi, \mathcal{T}, \mathcal{E}, C)\mathrm{d}\xi. \end{cases} \tag{24}$$

Using the approximation of the integrals of System (24) gives

$$\begin{cases} \mathcal{T}^{n+1} = \mathcal{T}^0 + \dfrac{\beta t_n^{\beta-1}(1-\varrho)}{\mathcal{M}(\varrho)}\mathcal{H}_1(t_n, \mathcal{T}^n, \mathcal{E}^n, C^n) \\ \quad + \dfrac{\varrho\beta}{\mathcal{M}(\varrho)\Gamma(\varrho)}\displaystyle\sum_{\varOmega=0}^{n}\int_{t_\varOmega}^{t_{\varOmega+1}} \xi^{\beta-1}(t_{n+1}-\xi)^{\varrho-1} \\ \quad \times \mathcal{H}_1(\xi, \mathcal{T}, \mathcal{E}, C)\mathrm{d}\xi, \\ \mathcal{E}^{n+1} = \mathcal{E}^0 + \dfrac{\beta t_n^{\beta-1}(1-\varrho)}{\mathcal{M}(\varrho)}\mathcal{H}_2(t_n, \mathcal{T}^n, \mathcal{E}^n, C^n) \\ \quad + \dfrac{\varrho\beta}{\mathcal{M}(\varrho)\Gamma(\varrho)}\displaystyle\sum_{\varOmega=0}^{n}\int_{t_\varOmega}^{t_{\varOmega+1}} \xi^{\beta-1}(t_{n+1}-\xi)^{\varrho-1} \\ \quad \times \mathcal{H}_2(\xi, \mathcal{T}, \mathcal{E}, C)\mathrm{d}\xi, \\ C^{n+1} = C^0 + \dfrac{\beta t_n^{\beta-1}(1-\varrho)}{\mathcal{M}(\varrho)}\mathcal{H}_2(t_n, \mathcal{T}^n, \mathcal{E}^n, C^n) \\ \quad + \dfrac{\varrho\beta}{\mathcal{M}(\varrho)\Gamma(\varrho)}\displaystyle\sum_{\varOmega=0}^{n}\int_{t_\varOmega}^{t_{\varOmega+1}} \xi^{\beta-1}(t_{n+1}-\xi)^{\varrho-1} \\ \quad \times \mathcal{H}_2(\xi, \mathcal{T}, \mathcal{E}, C)\mathrm{d}\xi. \end{cases} \tag{25}$$

Now, using the Lagrangian polynomial with piece-wise interpolation, we obtain the following:

$$\begin{cases} \mathcal{T}^{n+1} = \mathcal{T}^0 + \dfrac{\beta t_n^{\beta-1}(1-\varrho)}{\mathcal{M}(\varrho)}\mathcal{H}_1(t_n, \mathcal{T}^n, \mathcal{E}^n, C^n) \\ \quad + \dfrac{\beta(\Delta t)^\varrho}{\mathcal{M}(\varrho)\Gamma(\varrho+2)} \\ \quad \times \displaystyle\sum_{\varOmega=0}^{n}[t_\varOmega^{\beta-1}\mathcal{H}_1(t_\varOmega, \mathcal{T}^\varOmega, \mathcal{E}^\varOmega, C^\varOmega) \\ \quad \times ((n+1-\varOmega)^\varrho(n-\varOmega+2+\varrho) \\ \quad - (n-\varOmega)^\varrho(n-\varOmega+2+2\varrho)) \\ \quad - t_{\varOmega-1}^{\beta-1}\mathcal{H}_1(t_{\varOmega-1}, \mathcal{T}^{\varOmega-1}, \mathcal{E}^{\varOmega-1}, C^{\varOmega-1}) \\ \quad \times ((n-\varOmega+1)^{\varrho+1} - (n-\varOmega)^\varrho(n-\varOmega+1 \\ \quad + \varrho))], \\ \mathcal{E}^{n+1} = \mathcal{E}^0 + \dfrac{\beta t_n^{\beta-1}(1-\varrho)}{\mathcal{M}(\varrho)}\mathcal{H}_2(t_n, \mathcal{T}^n, \mathcal{E}^n, C^n) \\ \quad + \dfrac{\beta(\Delta t)^\varrho}{\mathcal{M}(\varrho)\Gamma(\varrho+2)} \\ \quad \times \displaystyle\sum_{\varOmega=0}^{n}[t_\varOmega^{\beta-1}\mathcal{H}_2(t_\varOmega, \mathcal{T}^\varOmega, \mathcal{E}^\varOmega, C^\varOmega) \\ \quad \times ((n+1-\varOmega)^\varrho(n-\varOmega+2+\varrho) \\ \quad - (n-\varOmega)^\varrho(n-\varOmega+2+2\varrho)) \\ \quad - t_{\varOmega-1}^{\beta-1}\mathcal{H}_2(t_{\varOmega-1}, \mathcal{T}^{\varOmega-1}, \mathcal{E}^{\varOmega-1}, C^{\varOmega-1}) \\ \quad \times ((n-\varOmega+1)^{\varrho+1} - (n-\varOmega)^\varrho(n-\varOmega+1 \\ \quad + \varrho))], \\ C^{n+1} = C^0 + \dfrac{\beta t_n^{\beta-1}(1-\varrho)}{\mathcal{M}(\varrho)}\mathcal{H}_3(t_n, \mathcal{T}^n, \mathcal{E}^n, C^n) \\ \quad + \dfrac{\beta(\Delta t)^\varrho}{\mathcal{M}(\varrho)\Gamma(\varrho+2)} \\ \quad \times \displaystyle\sum_{\varOmega=0}^{n}[t_\varOmega^{\beta-1}\mathcal{H}_3(t_\varOmega, \mathcal{T}^\varOmega, \mathcal{E}^\varOmega, C^\varOmega) \\ \quad \times ((n+1-\varOmega)^\varrho(n-\varOmega+2+\varrho) \\ \quad - (n-\varOmega)^\varrho(n-\varOmega+2+2\varrho)) \\ \quad - t_{\varOmega-1}^{\beta-1}\mathcal{H}_3(t_{\varOmega-1}, \mathcal{T}^{\varOmega-1}, \mathcal{E}^{\varOmega-1}, C^{\varOmega-1}) \\ \quad \times ((n-\varOmega+1)^{\varrho+1} - (n-\varOmega)^\varrho(n-\varOmega+1 \\ \quad + \varrho))]. \end{cases} \tag{26}$$

The presented numerical method for three cases has been proved that Adam–Bashforth method preserves accuracy in solving both linear and nonlinear problems involving

Table 2: Values of the parameters

Parameters	Values	Units
s_n	0.073	$\frac{\text{cell / µl}}{\text{day}}$
d_n	0.040	day^{-1}
d_e	0.06	day^{-1}
d_c	0.2	day^{-1}
k_n	0.001	day^{-1}
η	100	cells/μl
ϱ_n	0.41	
α_e	0.2	day^{-1}
$C_{\max}$	3×10^5	cells/µl
r_c	0.03	day^{-1}
γ_e	0.005	$\text{day}^{-1}\left(\frac{\text{cells}}{\mu\text{l}}\right)^{-1}$
γ_c	0.005	$\text{day}^{-1}\left(\frac{\text{cells}}{\mu\text{l}}\right)^{-1}$

fractional or fractal-fractional order derivatives (see details in the study by Zabidi *et al.* [59]).

5 Numerical simulations

For simulations, we consider the initial values for state variables along with parameter values from Table 2. The parameter values are also given in Table 2 and initial conditions are taken from the study of Moore and Li [55].

$$\mathcal{T}(0) = 1{,}510\,; \quad \mathcal{E}(0) = 20; \quad \mathcal{C}(0) = 10{,}000\,,$$

where all the initial values are considered in cells/µl.

Here, first, we use the numerical scheme for power-law kernel given in Eq. (19) to plot the approximate results for the proposed model in Figures 1–3, respectively. For plotting, we assign the values to fractal order as $\beta = 0.99$

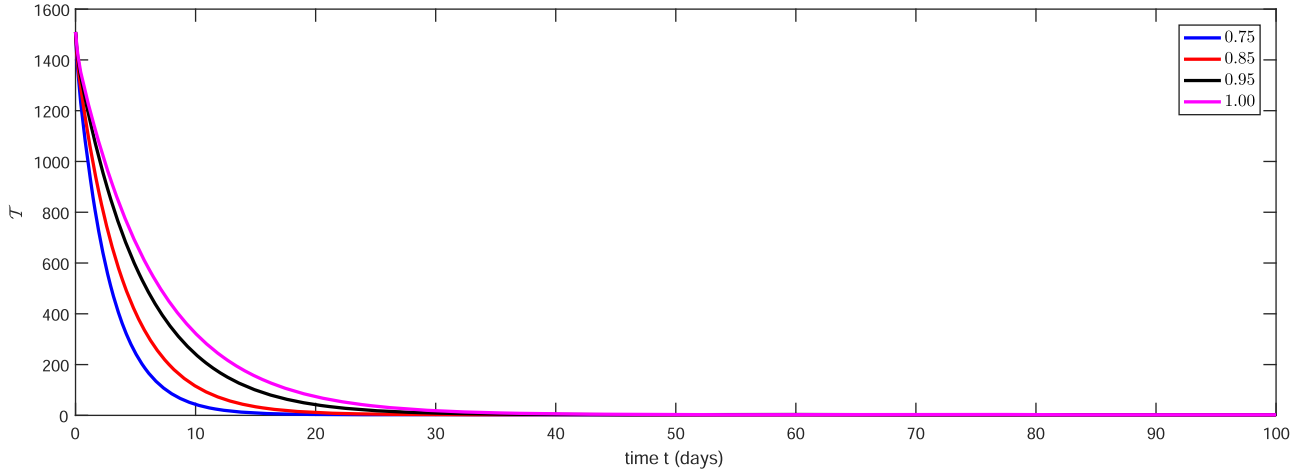

Figure 1: Graphical illustration for the naive $\mathcal{T}$ cells using Model (3) for $\varrho = 0.75, 0.85, 0.95, 1$ and $\beta = 0.99$.

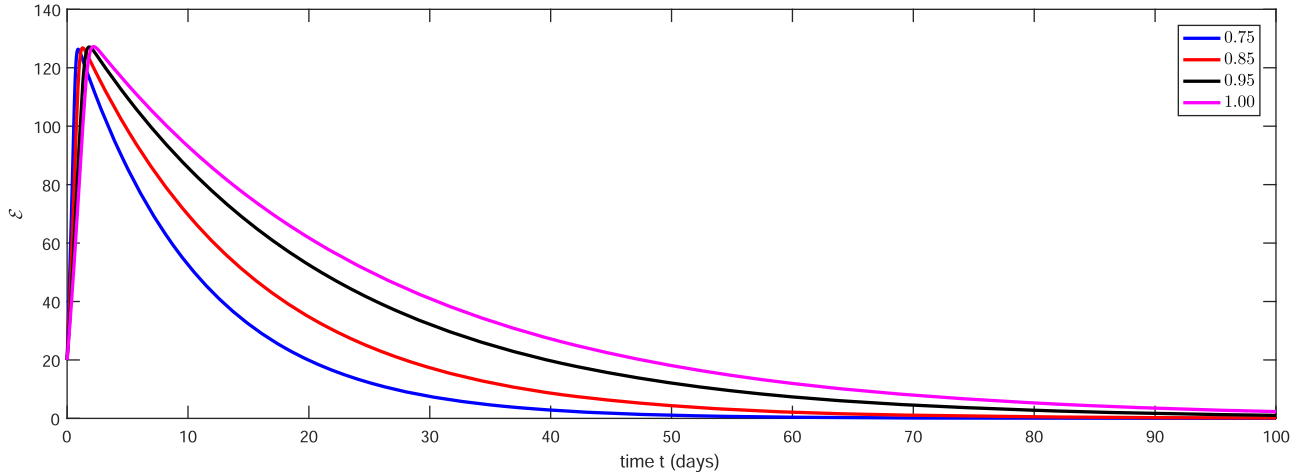

Figure 2: Graphical illustration for the effector $\mathcal{E}$ cells specific to CML using Model (3) for $\varrho = 0.75, 0.85, 0.95, 1$ and $\beta = 0.99$.

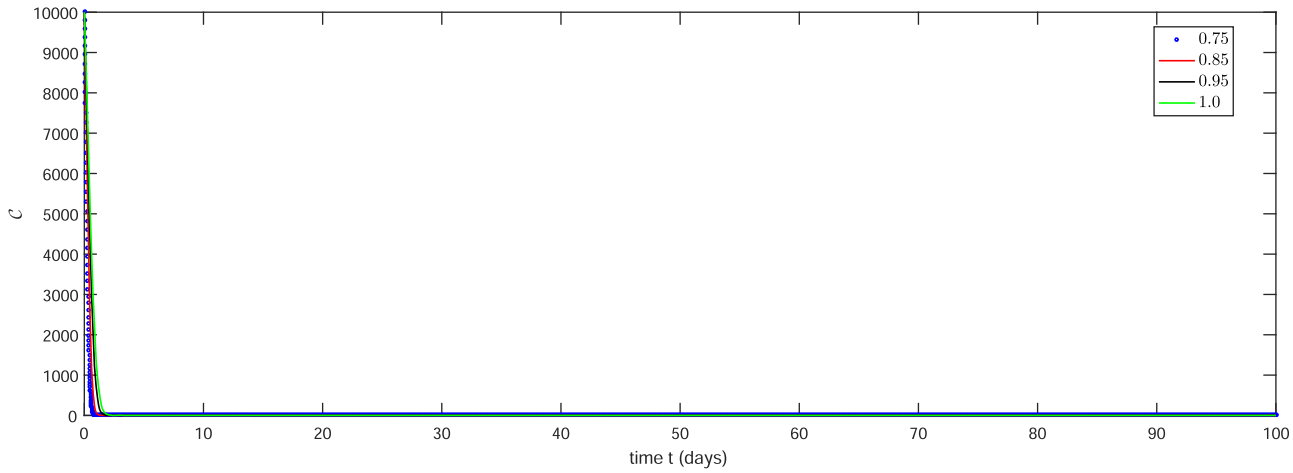

Figure 3: Graphical illustration for the CML cancer cells C using Model (3) for $\varrho = 0.75, 0.85, 0.95, 1$ and $\beta = 0.99$.

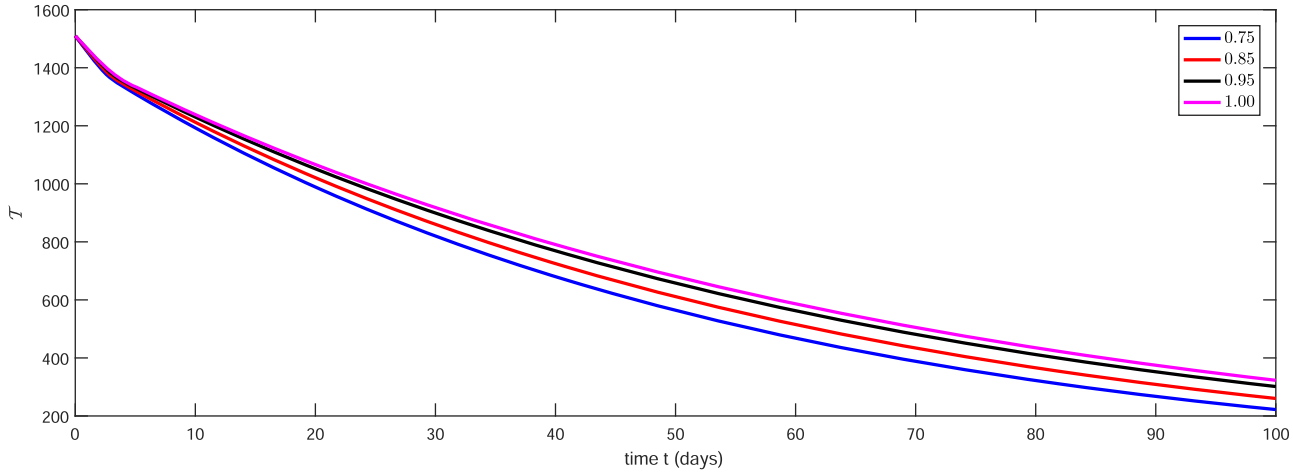

Figure 4: Graphical illustration for the naive $\mathcal{T}$ cells using Model (4) for $\varrho = 0.75, 0.85, 0.95, 1$ and $\beta = 0.99$.

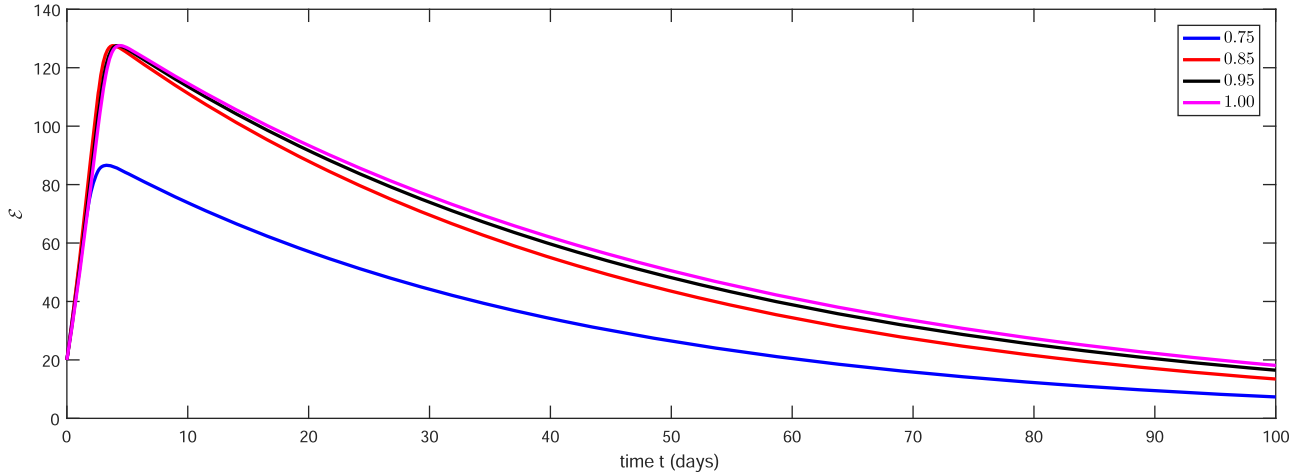

Figure 5: Graphical illustration for the effector $\mathcal{E}$ cells specific to CML using Model (4) for $\varrho = 0.75, 0.85, 0.95, 1$ and $\beta = 0.99$.

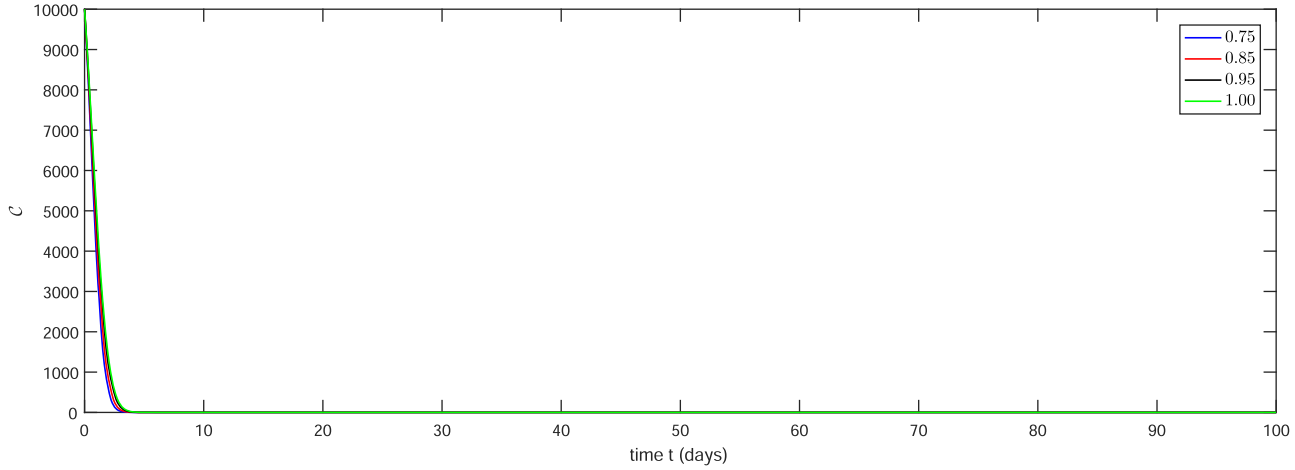

Figure 6: Graphical illustration for the CML cancer cells C using Model (4) for $\varrho = 0.75, 0.85, 0.95, 1$ and $\beta = 0.99$.

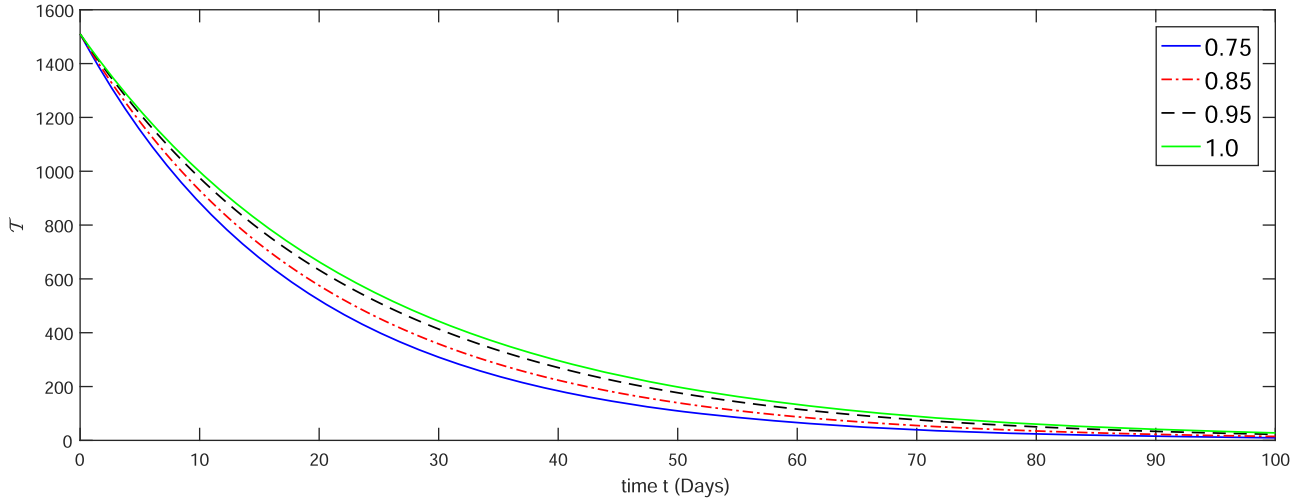

Figure 7: Graphical illustration for $\mathcal{T}$ cells using Model (5) for $\varrho = 0.75, 0.85, 0.95, 1$ and $\beta = 0.99$.

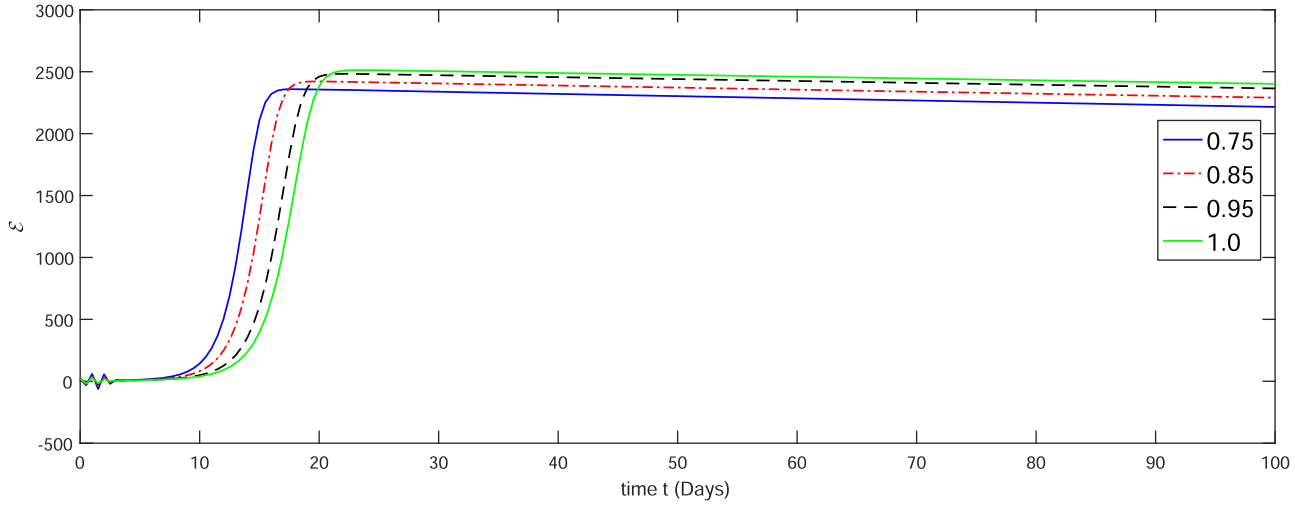

Figure 8: Graphical illustration for the effector $\mathcal{E}$ cells specific to CML using Model (5) for $\varrho = 0.75, 0.85, 0.95, 1$ and $\beta = 0.99$.

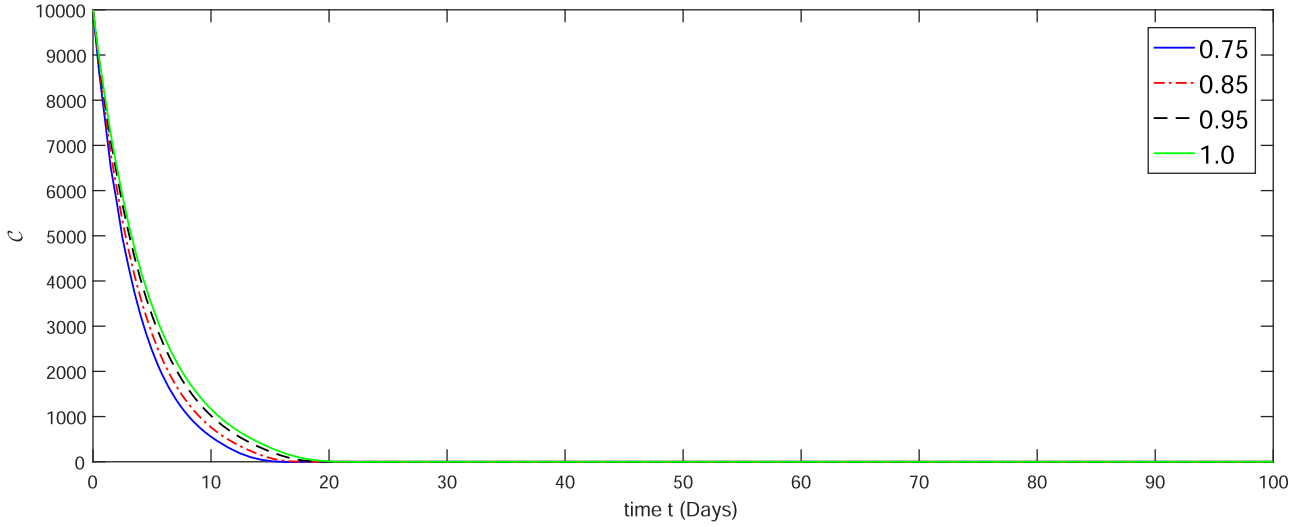

Figure 9: Graphical illustration for the CML cancer cells C using Model (5) for $\varrho = 0.75, 0.85, 0.95, 1$ and $\beta = 0.99$.

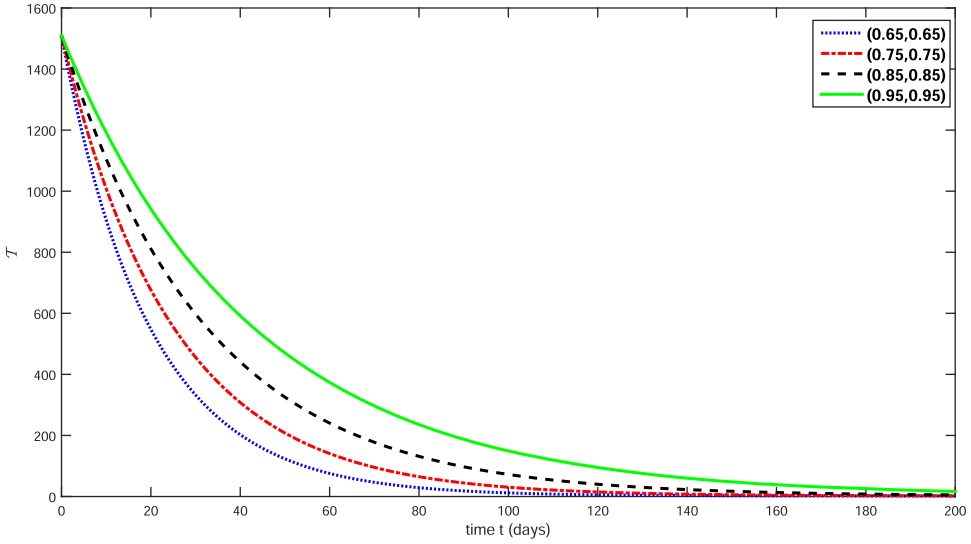

Figure 10: Graphical illustration for the $\mathcal{T}$ cells using Model (3) for different values of ϱ and β.

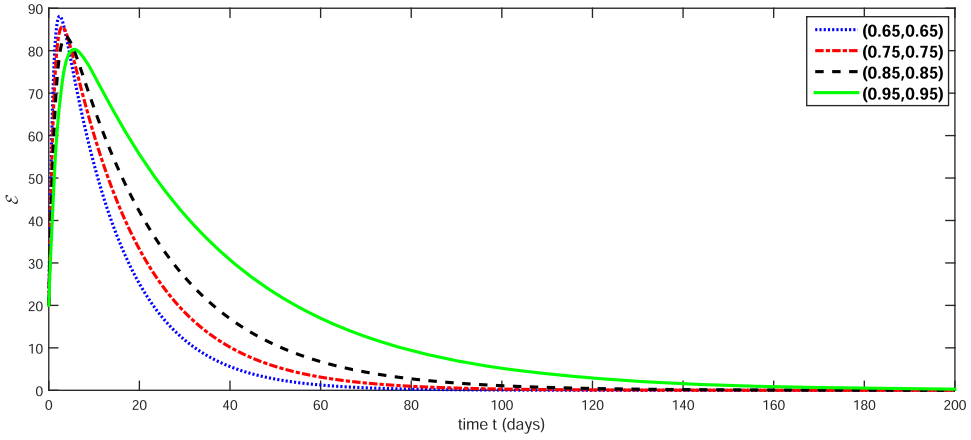

Figure 11: Graphical illustration for for the effector $\mathcal{E}$ cells specific to CML using Model (3) for different values of ϱ and β.

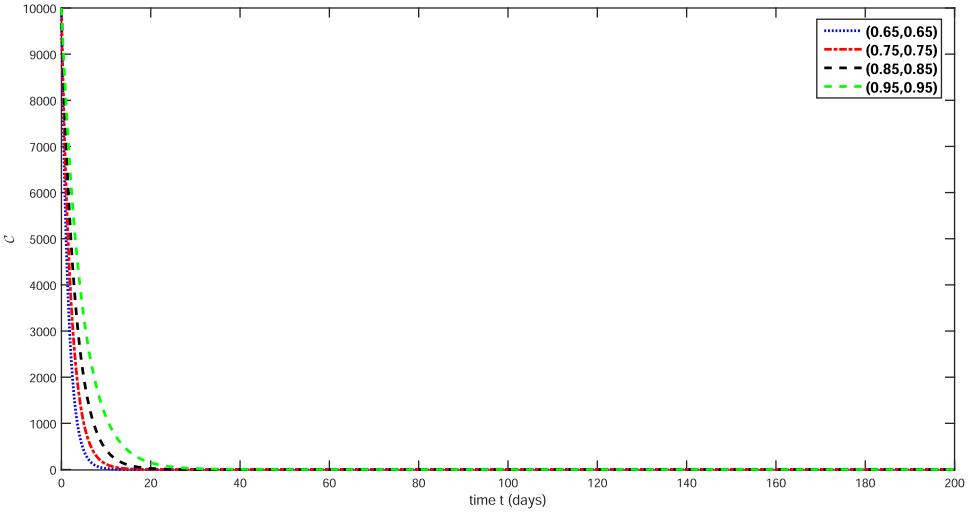

Figure 12: Graphical illustration for the CML cancer cells C using Model (3) for different values of ϱ and β.

and simulate the results through power-law algorithm for different fractional-order ϱ = 0.75, 0.85, 0.95, and 1. Using the given values of Table 2, we plot the graphs of approximate results obtained in Eqs. (23) and (26) for the considered model and obtain the graphs for Caputo Fabrizio and Atangana-Baleanu-Caputo case in Figures 4–6 and Figures 7–9, respectively. From Figures 1–3, we see that when naive T-cells are exposed to professional antigen-presenting cell (APC), then the number of naive T-cells are going to decreasing in approximately 1 month. As a result, the population of the effector T-cells specific to CML rapidly increases up to 5 days but later rebound, and the population of CML cancer cells rapidly decreases about in 1 day. From Figures 4–6, we note that the population of naive T-cells is steadily decreasing, resulting in a rise in the population of CML-specific effector T-cells up to 6 days but later rebounding and gradually decreasing in 4 months; the population of CML cancer is also decreasing. From Figures 7–9, we analyze that the population of naive T-cells decreases more steadily. As a result, the effector T-cell population increases and the CML cancer cell population gradually decreases. We see that the information given by the graphs of Mittag–Leffler kernel are more realistic than Caputo–Fabrizo type and power-law type for different fractional-order. By comparing the graphs obtained in the study by Moore and Li [55] with the plots for the fractal-fractional order model, it is clear that variation of the fractal-fractional order and control parameters can capture more complexities as compared to fractional differential operators.

Here, we present some plots for FFD operators with power-law kernel corresponding to different values of ϱ and β in Figures 10–12, respectively.

6 Discussion and conclusion

In this article, under newly proposed differentials and integral operators, we have investigated the mathematical model of the relationship between CML and T-cells. We have derived the results for the existence and uniqueness of the solution of the proposed model. In general, we have presented three numerical schemes with the use of Lagrangian polynomial piece-wise interpolation for the solution of the model under Caputo, Caputo–Fabrizio, and Atangana–Baleanu fractal-fractional operator. The first one is related to the power-law type kernel, the second one is concerned with the exponential-decay-type kernel, and the last one is related to the Mittag–Leffler-type kernel. We have presented the numerical results for fractional order ϱ = 0.75, 0.8, 0.95, 1 and fractal order β = 0.99. If ϱ = 1 and β = 1, then we recover the results of the ordinary operators from these operators. The increase and decrease of the compartments of the proposed model are due to varying fractional order. As we see in simulations, the fractional order has a great impact on the fractal dimension. The researchers also studied the influence of the fractal dimension on the fractional orders in several papers. From the figures, we have concluded that modeling with the Atangana–Baleanu operator is better than the Caputo and Caputo–Fabrizio because the dynamics of the proposed model obtained through the Atangana–Baleanu operator is more realistic than the other two differential operators. The Atangana–Baleanu fractal-fractional operator is thus the better choice for any dynamic model that does not predict by ordinary differential operators to study complex behavior. Furthermore, one can extend the current work to study

chaotic attractors and more complex behavior under different fractal and fractional operators of variable orders. In the future, young researchers can investigate different fractal-fractional differential operators in fuzzy sense, which is a more popular applicable area of research in the current time. Furthermore, the qualitative analysis of fractal-fractional differential operators can be investigated using newly established fixed point theorems. Also, spectral, collocations, and spline method of numerical analysis can be extended to investigate the said area.

Acknowledgments: Prince Sultan University is appreciated for APC and support through TAS research lab.

Funding information: Prince Sultan University is appreciated for APC and support through TAS research lab.

Author contributions: Kamal Shah has edited revised the paper. Shabir Ahmad has written the initial dradt. Aman Ullah included literature. Thabet Abdeljawad edited the final version of the paper. All authors have accepted responsibility for the entire content of this manuscript and approved its submission.

Conflict of interest: The authors state no conflict of interest.

Data availability statement: All data generated or analysed during this study are included in this published article.

References

[1] Machado JT, Kiryakova V, Mainardi F. Recent history of fractional calculus. Commun Nonl Sci Numer Simul. 2011;16(3):1140–53.
[2] AlBaidani MM, Aljuaydi F, Alharthi NS, Khan A, Ganie AH. Study of fractional forced KdV equation with Caputo–Fabrizio and Atangana-Baleanu-Caputo differential operators. AIP Adv. 2024;14(1):015340.
[3] Ferrari AL, Gomes MCS, Aranha ACR, Paschoal SM, De Souza Matias G, et al. Mathematical modeling by fractional calculus applied to separation processes. Separ Purifi Tech. 2024;2024:126310.
[4] Baleanu D, Hedayati V, Rezapour S, Al Qurashi MM. On two fractional differential inclusions. Springer Plus. 2016;5:1–15.
[5] Baleanu D, Ghafarnezhad K, Rezapour S, Shabibi M. On the existence of solutions of a three steps crisis integro-differential equation. Adv Diff Equ. 2018;2018(1):1–20.
[6] Rezapour S, Imran A, Hussain A, Martínez F, Etemad S, Kaabar MK. Condensing functions and approximate endpoint criterion for the existence analysis of quantum integro-difference FBVPs. Symmetry. 2021;13(3):469.
[7] Baleanu D, Mohammadi H, Rezapour S. On a nonlinear fractional differential equation on partially ordered metric spaces. Adv Diff Equ. 2013;2013:1–10.
[8] Baleanu D, Etemad S, Mohammadi H, Rezapour S. A novel modeling of boundary value problems on the glucose graph. Commun Nonl Sci Numer Simul. 2021;100:105844.
[9] Jamil S, Farman M, Akgül A, Saleem MU, Hincal E, El Din SM. Fractional order age dependent Covid-19 model: an equilibria and quantitative analysis with modeling. Results Phys. 2023;53:106928.
[10] Farman M, Shehzad A, Nisar KS, Hincal E, Akgül A, Hassan AM. Generalized Ulam-Hyers-Rassias stability and novel sustainable techniques for dynamical analysis of global warming impact on ecosystem. Scientific Reports. 2023;13(1):22441.
[11] Batool M, Farman M, Ahmad A, Nisar KS. Mathematical study of polycystic ovarian syndrome disease including medication treatment mechanism for infertility in women. AIMS Public Health. 2024;11(1):19–35.
[12] Xu C, Farman M, Shehzad A. Analysis and chaotic behavior of a fish farming model with singular and non-singular kernel. Int J Biomath. 2023;2023:2350105.
[13] Farman M, Ahmad A, Zehra A, Nisar KS, Hincal E, Akgül A. Analysis and controllability of diabetes model for experimental data by using fractional operator. Math Comput Simul. 2024;218:133–48.
[14] Khan H, Alam K, Gulzar H, Etemad S, Rezapour S. A case study of fractal-fractional tuberculosis model in China: existence and stability theories along with numerical simulations. Math Comput Simul. 2022;198:455–73.
[15] Akgül A. A novel method for a fractional derivative with non-local and non-singular kernel. Chaos Solitons Fractals. 2018;114:478–82.
[16] Akgül EK. Solutions of the linear and nonlinear differential equations within the generalized fractional derivatives. Chaos Interdiscipl J Nonl Sci. 2019;29(2):023108.
[17] Tuan NH, Mohammadi H, Rezapour S. A mathematical model for COVID-19 transmission by using the Caputo fractional derivative. Chaos Solitons Fractals. 2020;140:110107.
[18] Alderremy AA, Gómez-Aguilar JF, Aly S, Saad KM. A fuzzy fractional model of coronavirus (COVID-19) and its study with Legendre spectral method. Results Phys. 2021;21:103773.
[19] Pandey P, Chu YM, Gómez-Aguilar JF, Jahanshahi H, Aly AA. A novel fractional mathematical model of COVID-19 epidemic considering quarantine and latent time. Results Phys. 2021;26:104286.
[20] Atangana A, Akgül A, Owolabi KM. Analysis of fractal fractional differential equations. Alexandria Eng J. 2020;59(3):1117–34.
[21] Chen W. Time-space fabric underlying anomalous diffusion. Chaos Solitons Fractals. 2006;28:923–31.
[22] Atangana A, Baleanu D. New fractional derivatives with non-local and non-singular kernel: theory and application to heat transfer model. Therm Sci. 2016;20(2):763–71.
[23] Atangana A, Akgül A. Can transfer function and Bode diagram be obtained from Sumudu transform. Alexandria Eng J. 2020;59:1971–84.
[24] Kumar D, Singh J, Al Qurashi M, Baleanu D. A new fractional SIRS-SI malaria disease model with application of vaccines, antimalarial drugs, and spraying. Adv Diff Equ. 2019;2019(1):1–9.
[25] Srivastava HM, Dubey VP, Kumar R, Singh J, Kumar D, Baleanu D. An efficient computational approach for a fractional-order biological population model with carrying capacity. Chaos Solitons Fractals. 2020;138:109880.
[26] Kumar S, Kumar R, Singh J, Nisar KS, Kumar D. An efficient numerical scheme for fractional model of HIV-1 infection of CD4+ T-

cells with the effect of antiviral drug therapy. Alexandr Eng J. 2020;59(4):2053–64.
[27] Singh J. Analysis of fractional blood alcohol model with composite fractional derivative. Chaos Solitons Fractals. 2020;140:110127.
[28] Ahmad S, Ullah A, Arfan M, Shah K. On analysis of the fractional mathematical model of rotavirus epidemic with the effects of breastfeeding and vaccination under Atangana-Baleanu (AB) derivative. Chaos Solitons Fractals. 2020;140:110233.
[29] Al Elaiw A, Hafeez F, Jeelani MB, Awadalla M, Abuasbeh K. Existence and uniqueness results for mixed derivative involving fractional operators. AIMS Math. 2023;8:7377–93.
[30] Jeelani MB. Stability and computational analysis of COVID-19 using a higher order galerkin time discretization scheme. Adv Appl Stat. 2023;86(2):167–206.
[31] Moumen A, Shafqat R, Alsinai A, Boulares H, Cancan M, Jeelani MB. Analysis of fractional stochastic evolution equations by using Hilfer derivative of finite approximate controllability. AIMS Math. 2023;8:16094–114.
[32] Khan AA, Amin R, Ullah S. Numerical simulation of a Caputo fractional epidemic model for the novel coronavirus with the impact of environmental transmission. Alexandria Eng J. 2022;61:5083–95.
[33] Kumar S, Ahmadian A, Kumar R, Kumar D, Singh J, Baleanu D, et al. An efficient numerical method for fractional SIR epidemic model of infectious disease by using Bernstein wavelets. Math. 2020;8(4):558.
[34] Abdo MS, Shah K, Wahash HA, Panchal SK. On a comprehensive model of the novel coronavirus (COVID-19) under Mittag–Leffler derivative. Chaos Solitons Fractals. 2020;135:109867.
[35] Zhou Y, Zhang Y. Noether symmetries for fractional generalized Birkhoffian systems in terms of classical and combined Caputo derivatives. Acta Mechanica. 2020;231(7):3017–29.
[36] Atangana A, Qureshi S. Modeling attractors of chaotic dynamical systems with fractal-fractional operators. Chaos Solitons Fractals. 2019;123:320–37.
[37] Sabir Z, Munawar M, Abdelkawy MA, Raja MA, Ünlü C, Jeelani MB, et al. Numerical investigations of the fractional-order mathematical model underlying immune-chemotherapeutic treatment for breast cancer using the neural networks. Fractal Fract. 2022;6:184.
[38] Sumelka W, Luczak B, Gajewski T, Voyiadjis GZ. Modelling of AAA in the framework of time-fractional damage hyperelasticity. Int J Solid Struct. 2020;206:30–42.
[39] Sun H, Meerschaert MM, Zhang Y, Zhu J, Chen W. A fractal Richard's equation to capture the non-Boltzmann scaling of water transport in unsaturated media. Adv Water Res. 2013;52:292–5.
[40] Atangana A, Goufo EF. Some misinterpretations and lack of understanding in differential operators with no singular kernels. Open Physics. 2020;18(1):594–612.
[41] Atangana A. Fractal-fractional differentiation and integration: connecting fractal calculus and fractional calculus to predict complex system. Chaos Solitons Fractal. 2017;102:396–406.
[42] Ahmad S, Ullah A, Akgül A, De la Sen M. Study of HIV disease and its association with immune cells under nonsingular and nonlocal fractal-fractional operator. Complexity. 2021;2021:1–2.
[43] Atangana A, Qureshi S. Modeling attractors of chaotic dynamical systems with fractal-fractional operators. Chaos Solitons Fractals. 2019;123:320–37.
[44] Arfan M, Shah K, Ullah A, Shutaywi M, Kumam P, Shah Z. On fractional order model of tumor dynamics with drug interventions under nonlocal fractional derivative. Results Phys. 2021;21:103783.
[45] Shah K, Arfan M, Mahariq I, Ahmadian A, Salahshour S, Ferrara M. Fractal-Fractional Mathematical Model Addressing the Situation of Corona Virus in Pakistan. Results Phys. 2020;19:103560.
[46] Tatom FB. The relationship between fractional calculus and fractals. Fractals. 1995;3(1):217–29.
[47] Rezapour S, Etemad S, Mohammadi H. A mathematical analysis of a system of Caputo–Fabrizio fractional differential equations for the anthrax disease model in animals. Adv Diff Equ. 2020;2020(1):481.
[48] O'Malley JRE. Differential equations and mathematical biology. SIAM Review. 2010;52(3):586.
[49] Kumar D, Singh J, editors. Fractional calculus in medical and health science. New York: CRC Press; 2020.
[50] Faderl S, Talpaz M, Estrov Z, Kantarjian HM. Chronic myelogenous leukemia: biology and therapy. Ann Int Med. 1999;131(3):207–19.
[51] Deininger MW, Goldman JM, Melo JV. The molecular biology of chronic myeloid leukemia. Blood J Am Soc Hematol. 2000;96(10):3343–56.
[52] Deininger MW, O'brien SG, Ford JM, Druker BJ. Practical management of patients with chronic myeloid leukemia receiving imatinib. J Clin Onco. 2003;21(8):1637–47.
[53] Sawyers CL. Chronic myeloid leukemia. N Engl J Med 1999;340(17):1330–40.
[54] Nanda S, Moore H, Lenhart S. Optimal control of treatment in a mathematical model of chronic myelogenous leukemia. Math Biosci. 2007;210(1):143–56.
[55] Moore H, Li NK. A mathematical model for chronic myelogenous leukemia (CML) and T cell interaction. J Theore Bio. 2004;227(4):513–23.
[56] Ali Z, Rabiei F, Hosseini K. A fractal-fractional-order modified Predator-Prey mathematical model with immigrations. Math Comput Simul. 2023;207:466–81.
[57] Ali Z, Rabiei F, Shah K, Khodadadi T. Fractal-fractional order dynamical behavior of an HIV/AIDS epidemic mathematical model. The Euro Phy J Plus. 2021;136(1):36.
[58] Khan MA, Atangana A. Numerical methods for fractals-fractional differential equations and engineering: simulations and modelings. New York: CRC Press; 2022.
[59] Zabidi NA, Abdul Majid Z, Kilicman A, Rabiei F. Numerical solutions of fractional differential equations by using fractional explicit Adams method. Mathematics. 2020;8(10):1675.
[60] Istratescu VI. Fixed point theory: an introduction. New York: Springer Science & Business Media; 2001.